

# SPACE DECOUPLED LOAD FLOW ANALYSIS

A project submitted to  
the Department of Electrical and Electronic Engineering,  
Bangladesh University of Engineering and Technology  
in partial fulfilment of the requirements for the degree of  
Master of Engineering (Electrical and Electronic)

by

MD. ABUL KALAM

April 1994



Department of Electrical and Electronic Engineering  
Bangladesh University of Engineering and Technology

Dhaka, Bangladesh.



#87389#

v R v  
623.81  
1994  
ABU

### Declaration

This work was done by me and it has not been submitted elsewhere for the award of any degree or diploma.

Countersigned

Signature of the Candidate

S. Shahnawaz Ahmed

(Dr. S. Shahnawaz Ahmed)

Supervisor

Md. Abul Kalam  
21/4/94

(Md. Abul Kalam)

Approval

The project titled  
Space Decoupled Load Flow Analysis

by

Md. Abul Kalam

Roll : 891326F

has been accepted as satisfactory in partial fulfilment of the requirements for the degree of Master of Engineering (Electrical and Electronic).

Board of Examiners :

(i)

 21/04/1994


(Dr. S. Shahnawaz Ahmed)

Associate Professor

Department of Electrical and  
Electronic Engineering, BUET.

Chairman  
(Supervisor)

(ii)

 21.4.94.

(Dr. Syed Fazl-i Rahman)

Professor and Head

Department of Electrical and  
Electronic Engineering, BUET.

Member

(iii)

 21.4.94

(Dr. Enamul Basher)

Associate Professor

Department of Electrical and  
Electronic Engineering, BUET.

Member

## Acknowledgements

It is a matter of great pleasure on the part of the author to acknowledge his profound gratitude to his Supervisor Dr. S. Shahnawaz Ahmed for his support, advice, valuable guidance, assistance and his constant encouragement throughout the progress of this research work.

The author also acknowledges his deep sense of gratitude to Dr. Syed Fazl-i Rahman, Professor and Head and Dr. Enamul Basher, Associate Professor of the Department of Electrical and Electronic Engineering, BUET for showing interest and providing support and encouragement in this work.

The author also wishes to express his sincere thanks to the Director and the staff of BUET Computer Centre for their cooperation.

## Abstract

A decomposed load flow analysis method has been proposed in which the active and reactive Jacobian matrices of the fast decoupled algorithm are also space decoupled i.e. intersubsystem coupling through tie lines has been considered only in the diagonal elements of subsystems. This enables parallel solution in all the subsystems for a system of any size and avoids separate computations involving tie line models saving extra CPU time and memory. Also the proposed technique avoids the singularity problem of subsystem active Jacobian matrices without requiring assignment of temporary slack buses in the subsystems. The performance of the proposed method has been extensively investigated considering various operating conditions and decomposition schemes of IEEE 14, 30, 57 bus systems and a practical 81 bus (BPDB) system. Also the performance has been compared against the integrated fast decoupled load flow solution of the same systems without decomposing them. Sparsity has been exploited in both the decomposed and the integrated methods.

## LIST OF PRINCIPAL SYMBOLS AND ABBREVIATIONS

$P_{Gi}$	Specified active power generation at bus $i$ .
$P_{Li}$	Specified active load at bus $i$ .
$P_i$	Specified active power injection at a P-V or P-Q bus $i$ and equal to $(P_{Gi} - P_{Li})$ .
$g_{ik}$	Series conductance of the branch $i$ - $k$ .
$b_{ik}$	Series susceptance of the branch $i$ - $k$ .
$\theta_{ik}$	Difference between phase angles of buses $i$ and $k$ i.e. $\theta_i - \theta_k$ .
$Q_{Gi}$	Specified reactive power generation at bus $i$ .
$Q_{Li}$	Specified reactive load at bus $i$ .
$Q_i$	Specified reactive power injection at bus $i$ and equal to $(Q_{Gi} - Q_{Li})$ .
$s_{ik}$	Half of the charging susceptance in line $i$ - $k$ .
$\Delta P_i$	Active power mismatch at bus $i$ .
$\Delta Q_i$	Reactive power mismatch at bus $i$ .
$[J_{P\theta}]_{ii}$	Active Jacobian matrix of subsystem $i$ .
$[J_{Q\theta}]_{ii}$	Reactive Jacobian matrix of subsystem $i$ .
NR	Newton-Raphson.
FD	Fast Decoupled.
IEEE	Institute of Electrical and Electronics Engineers.
CPU	Central Processing Unit.
IBM	International Business Machines.
BPDB	Bangladesh Power Development Board.

## CONTENTS

	page
<b>CHAPTER 1 INTRODUCTION</b>	
1.1 General Considerations	2
1.2 Review of Previous Works	3
1.3 Purpose of the Present Project	5
1.4 Organisation of the Report	6
<b>CHAPTER 2 OVERVIEW OF INTEGRATED LOAD FLOW ANALYSIS</b>	
2.1 Introduction	9
2.2 Fast Decoupled Newton-Raphson Load Flow Analysis	11
2.3 Bifactorization of Sparse Jacobian matrices	17
2.4 Conclusions	20
<b>CHAPTER 3 DECOMPOSED LOAD FLOW ANALYSIS THROUGH SPACE DECOUPLING</b>	
3.1 Introduction	23
3.2 Proposed Technique of Space Decoupling	23
3.3 Flow Chart for the Proposed Decomposed Load Flow Analysis	30
3.4 Conclusions	32

## CHAPTER 4 PRESENTATION OF RESULTS

4.1	Introduction	34
4.2	Study of IEEE 14 Bus System	35
4.3	Study of IEEE 30 Bus System	40
4.4	Study of IEEE 57 Bus System	45
4.5	Study of BPDB 81 Bus System	50
4.6	Analysis of the Decomposed Method's Convergence Characteristics	55
4.7	Comparison of CPU Time and Memory Requirement of the Decomposed and Integrated Methods	63
4.8	Conclusions	69

## CHAPTER 5 CONCLUSIONS

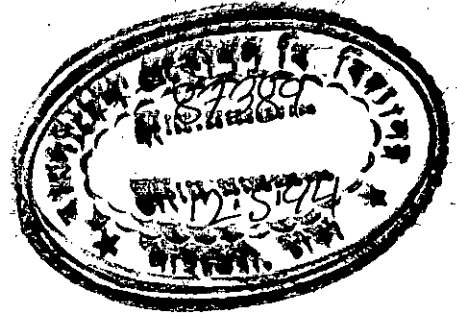
5.1	Conclusions	73
5.2	Suggestions for Further Research	75

REFERENCES	77
------------	----

## APPENDICES

APPENDIX A	IEEE 14 BUS SYSTEM DATA	A-1
APPENDIX B	IEEE 30 BUS SYSTEM DATA	B-1
APPENDIX C	IEEE 57 BUS SYSTEM DATA	C-1
APPENDIX D	BPDB 81 BUS GRID SYSTEM DATA	D-1





**CHAPTER 1**  
**INTRODUCTION**

## 1.1 General Considerations

Load flow analysis is a digital computer method of solving a set of nonlinear algebraic equations for the unknown bus voltage magnitudes, phase angles and line flows in a power system in the steady state when the power injection and/or voltage magnitudes are specified at an equal number of buses. Load flow also known as power flow solution is necessary for a number of other application functions in modern power system analysis. These are, for instances, (i) system planning i.e. analysing the effects of addition of generation and transmission facilities, (ii) system operation like economic dispatch (generation scheduling) and security analysis i.e. to foresee the effects of contingencies like loss of a generator or outage of a transmission line and (iii) transient stability analysis requiring a prefault run of the load flow solution for setting the initial conditions. Therefore it is important that the load flow solution must be fast enough so that the subsequent computations can be accomplished and decisions be implemented within the stipulated time specially for real time operation and control of a present day's sophisticated power system. But with the continued growth in demand for electricity and hence an increase in system size as well as a tendency to interconnect two or more areas or utilities, the dimensionality of

the load flow and the other power system problems increases. So to reduce the on-line time for the control actions a recent approach being adopted by the power utilities is decentralized control with distributed computer system. In this approach a system is divided into a number of already existent areas or suitably chosen subsystems and then the problem is solved for all the areas parallelly on respective computers followed by a coordination on one of the area computers or a separate central computer.

## 1.2 Review of Previous Works

A great deal of research effort has been put into evolving efficient power flow solution algorithms<sup>1-2</sup>. The first one was the slowly convergent Gauss-Seidal iterative method based on the sparse bus admittance matrix  $[Y_{bus}]$  without requiring its inversion. Then the transition was through the bus impedance matrix  $[Z_{bus}]$  method which takes relatively less number of iterations but requires the full inverse of the bus admittance matrix or a complicated  $[Z_{bus}]$  building algorithm. The finally evolved one was the Jacobian  $[J]$  matrix based basic Newton-Raphson (N-R) method and its subsequent improved versions are like the decoupled N-R (separation of active and reactive variables) and the fast decoupled (constant active and reactive Jacobian matrices) N-R methods. By now the fast decomposed

N-R algorithm is the most efficient one in terms of iterations, computation time and memory requirements. However, all these algorithms solve a system in a single piece and hence termed integrated load flow analysis.

But with an increase in the system size the integrated approach can not satisfy the on-line CPU time requirement despite making use of the fast decoupling and sparse matrix factorization<sup>3</sup> techniques instead of explicit inversion. To overcome this drawback of the integrated approach three major decomposed load flow analysis algorithms have been proposed in the literature<sup>4-6</sup>. These are respectively based on the basic N-R<sup>4</sup> and the fast decoupled N-R<sup>5-6</sup>.

In the decomposed basic N-R method each subsystem's Jacobian is formed excluding the admittances of the tie lines between subsystems and its bus voltages and phase angles are solved for separately. Then the subsystems' solutions are modified in each iteration through a six step algorithm considering a tie line current vector and the bus impedance submatrices for the subsystem and tie lines. Though a convergence close to that of the integrated method is expected the main drawbacks of this method are use of

both Jacobian and bus impedance matrices and extra CPU time for tie line coordination.

In the fast decoupled decomposed methods<sup>5-6</sup> a temporary slack bus (TSB) is assigned in each subsystem excepting the one containing the original system slack bus to overcome the singularity of the subsystem Jacobian matrices specially the active Jacobian matrices. Though a convergence same as that of the integrated method was reported, the way the subsystem solutions are coordinated taking into account the TSB's and tie lines is complicated requiring explicit inverses of some of the matrices and a high amount of data transfer between subsystem and coordinating computers. Moreover, one of the methods<sup>6</sup> required special way of tearing a system and assigning TSB's.

### 1.3 Purpose of the Present Investigation

It appears that the existing decomposed load flow algorithms<sup>4-6</sup> suffer from the drawbacks of complicated and time consuming computations and excessive data transfer due to a separate coordination step in each iteration considering the tie line and/or temporary slack bus (TSB) models. The present research project has the following objectives.

- i) To improve the computational performance of the decomposed fast decoupled load flow analysis by including tie line admittances in diagonal elements of the subsystem Jacobian matrices and considering the tie line flows in the subsystem power mismatch vector. This will decouple the subsystems completely and eliminate the need of assigning TSB as well as separate coordination of the tie line models. All the subsystems' computations will go on parallelly and provide the final solution for voltage magnitudes and phase angles.
  
- ii) To compare the performance of the proposed decomposed load flow technique against that of the integrated method through extensive test on IEEE test systems and a practical grid system of the Bangladesh Power Development Board (BPDB).

#### 1.4 Organisation of the Report

The presentation of the material studied in the present research project is organised as follows.

Chapter 2 highlights the principles of the fast decoupled Newton-Raphson load flow for the integrated approach and the sparsity directed bifactorisation technique.

Chapter 3 provides the theory of the proposed decomposed load flow analysis using the fast decoupled N-R technique.

Chapter 4 presents a quantitative comparison of the solution and computational performance of the proposed decomposed technique against those of the integrated technique.

Chapter 5 provides a summary of the main results achieved in the present project and suggestions for further research.

The appendices include the data for various test systems.

**CHAPTER 2**  
**OVERVIEW OF INTEGRATED LOAD FLOW ANALYSIS**



## 2.1 Introduction

The formulation of the load flow analysis problem is nonlinear<sup>1</sup> though the power transmission network is linear. This is because of the fact that power is a product of voltage and current i.e. proportional to the square of the voltage when both voltage and current in an a.c. network are complex quantities having a magnitude and an angle in the polar coordinate. So the load flow analysis needs the solution of a set of nonlinear and transcendental algebraic equations. In the fast decoupled (FD) method, the most efficient algorithm for load flow analysis, the set of nonlinear equations are solved as two subsets and iteratively through successive linearisation by the Newton-Raphson technique with a suitable choice for the initial values of unknown voltage magnitudes and phase angles in the first iteration. One subset relates the changes in phase angles to the changes in calculated active powers from their specified values through a constant Jacobian matrix while it neglects the weak coupling between voltage magnitudes and active power changes. The other subset relates the changes in voltage magnitudes to the changes in calculated reactive powers from their specified values through a constant Jacobian matrix while it neglects the weak coupling between the phase angles and reactive power changes. As the

Jacobian matrices of the FD method are made constant i.e. dependent upon only network admittances taking advantage of the characteristics of a high voltage power transmission system, they need to be inverted only once prior to the start of iteration. However, due to the inherent sparse structure of a power network, the Jacobian matrices of a system are also sparse and stored and inverted through sparsity<sup>1</sup> exploited bifactorisation method instead of a conventional explicit matrix inversion method. This increases further the CPU time and memory saving of the fast decoupled method.

The mathematical model to be developed for load flow analysis requires a prior classification of the buses of a power system into three categories depending upon the known and unknown quantities at a bus. One of these is slack or swing ( $V-\theta$ ) bus with a generator connected to it and a specified voltage magnitude and zero phase angle. The purpose of the slack bus is to provide a reference for the phase angles of other buses while the voltage magnitudes at all the buses are with reference to the ground. Also as active and reactive powers at the slack bus are unknown, the generator connected to it can be used to supply the difference between the total of specified powers at other buses and the total of system

demand (load) and losses. The other two categories are respectively generation (P-V) and load (P-Q) buses. At each P-V bus active power injection and voltage magnitude are specified while reactive power and phase angle are to be determined. At each P-Q bus both active and reactive power injection are specified while the voltage magnitude and phase angle are to be determined. The term injection denotes the difference between the specified generation and the specified load of a bus.

## 2.2 Fast Decoupled Newton-Raphson Load Flow Analysis

The set of nonlinear and transcendental equations for buses with specified active power injection is given<sup>1,2</sup> as follows.

$$P_i = v_i^2 \sum_{k \in \alpha_i} g_{ik} + \sum_{k \in \alpha_i} v_i v_k (-g_{ik} \cos \theta_{ik} - b_{ik} \sin \theta_{ik}) \quad (2.1)$$

where,

- $i$  : 1, 2 .....No. of P-V and P-Q buses,
- $k \in \alpha_i$  : set of buses directly connected to bus  $i$  by a transmission line,
- $P_i$  : specified active power injection at a P-V or P-Q bus  $i$  and equal to  $(P_{Gi} - P_{Li})$
- $P_{Gi}$  : specified active power generation at bus  $i$ ,
- $P_{Li}$  : specified active load at bus  $i$ ,

- $g_{ik}$  : series conductance of the branch i-k,
- $b_{ik}$  : series susceptance of the branch i-k,
- $v_i$  : voltage magnitude at bus i,
- $\theta_{ik}$  : difference between phase angles of buses i and k  
i.e.  $\theta_i - \theta_k$

The set of equations for the buses with specified reactive power injection i.e. P-Q buses given<sup>1,2</sup> by

$$Q_i = -v_i^2 \sum_{k \in \alpha_i} (b_{ik} + s_{ik}) + \sum_{k \in \alpha_i} v_i v_k (-g_{ik} \sin \theta_{ik} + b_{ik} \cos \theta_{ik}) \quad (2.2)$$

where,

- $i$  : 1, 2 .....No. P-Q buses,
- $Q_i$  : specified reactive power injection at bus i and equal to  
( $Q_{Gi} - Q_{Li}$ ),
- $Q_{Gi}$  : specified reactive power generation at bus i,
- $Q_{Li}$  : specified reactive load at bus i,
- $s_{ik}$  : half of the charging susceptance in line i-k.

The other notations in equation (2.2) have the same meaning as those used for equation (2.1)

The nonlinear equations (2.1) and (2.2) are linearised by the Taylor's series expansion around an initial point ( $v^0, \theta^0$ ) and the

higher order terms are neglected to result in the following equations.

$$P_i = P_i (v^0, \theta^0) + \sum_{k \in \alpha_i} \frac{\partial P_i}{\partial \theta_k} (\theta_k - \theta_k^0) + \sum_{k \in \alpha_i} \frac{\partial P_i}{\partial v_k} (v_k - v_k^0) \quad (2.3)$$

$$Q_i = Q_i (v^0, \theta^0) + \sum_{k \in \alpha_i} \frac{\partial Q_i}{\partial \theta_k} (\theta_k - \theta_k^0) + \sum_{k \in \alpha_i} \frac{\partial Q_i}{\partial v_k} (v_k - v_k^0) \quad (2.4)$$

Since the changes in active powers due to changes in voltage magnitudes and the changes in reactive powers due to changes in the phase angles can be neglected, equations (2.3) and (2.4) can be rewritten as follows.

$$P_i - P_i (v^0, \theta^0) = \sum_{k \in \alpha_i} \frac{\partial P_i}{\partial \theta_k} (\theta_k - \theta_k^0)$$

$$\text{or, } \Delta P_i = \sum_{k \in \alpha_i} \frac{\partial P_i}{\partial \theta_k} \Delta \theta_k \quad (2.5)$$

$$Q_i - Q_i (v^0, \theta^0) = \sum_{k \in \alpha_i} \frac{\partial Q_i}{\partial v_k} (v_k - v_k^0)$$

$$\text{or, } \Delta Q_i = \sum_{k \in \alpha_i} \frac{\partial Q_i}{\partial v_k} \Delta v_k \quad (2.6)$$

In equation (2.5)  $\Delta P_i$  denotes the difference between specified and calculated active power injection i.e. active power mismatch at bus i. Similarly in equation (2.6)  $\Delta Q_i$  denotes the reactive

power mismatch. The notations  $\Delta\theta_k$  and  $\Delta v_k$  respectively denote the changes in phase angle and voltage magnitude from the initial values.

Equations (2.5) and (2.6) can be reformulated in matrix form for a generalized iterative sequence as follows.

$$[\Delta P_i]^{n+1} = [J_{P\theta}]^n [\Delta\theta]^{n+1} \quad (2.7)$$

$$[\Delta Q_i]^{n+1} = [J_{Qv}]^n [\Delta v]^{n+1} \quad (2.8)$$

where,

m : iteration number

$$[J_{P\theta}]^m = \left. \frac{\partial P(v, \theta)}{\partial \theta} \right|_{\substack{v = v^m \\ \theta = \theta^m}} \quad (2.9)$$

is the active Jacobian matrix in m-th iteration.

$$[J_{Qv}]^m = \left. \frac{\partial Q(v, \theta)}{\partial v} \right|_{\substack{v = v^m \\ \theta = \theta^m}} \quad (2.10)$$

is the reactive Jacobian matrix in m-th iteration.

$$\Delta P_i^{n+1} = P_i(v^{n+1}, \theta^{n+1}) - P_i(v^n, \theta^n) \quad (2.11)$$

$$\Delta Q_i^{n+1} = Q_i(v^{n+1}, \theta^{n+1}) - P_i(v^n, \theta^n) \quad (2.12)$$

$$[\Delta\theta]^{n+1} = [\theta]^{n+1} - [\theta]^n \quad (2.13)$$

$$[\Delta v]^{n+1} = [v]^{n+1} - [v]^n \quad (2.14)$$

In equations (2.11) and (2.12)  $P_i(v^n, \theta^n)$  and  $Q_i(v^n, \theta^n)$  respectively denotes the active and reactive powers calculated at bus  $i$  using equations (2.1) and (2.2) and substituting  $v^n$  and  $\theta^n$  for  $v$  and  $\theta$ .

The elements in active and reactive Jacobian matrices of equations (2.7) and (2.8) also depend upon the bus voltage magnitudes and phase angles and hence the matrices need to be formed and then inverted in each iteration. In the fast decoupled<sup>1,2</sup> method a number of simplifications and assumptions based on the physical characteristics of a high voltage power transmission network are applied to make the Jacobian matrices constant i.e. independent of voltage magnitudes and phase angles requiring only one time inversion before the iterative process. These are as follows.

- i) Equations (2.1) and (2.2) are divided by the corresponding voltage magnitude.
- ii) Bus voltage magnitudes are assumed at their nominal values i.e. 1.0 per unit.

iii) As the angle difference across transmission lines are small under normal loading conditions it is assumed that  $\sin\theta_{ik} \approx 0$  and  $\cos\theta_{ik} \approx 1.0$ .

iv) Resistance to reactive ratios of the branches i.e.  $r/x \ll 1$  so that the series resistance can be neglected in the susceptance terms i.e.  $b_{ik} \approx 1/x_{ik}$ .

The application of these simplifications and assumptions make the elements of Jacobian matrices constant as in Table 2.1.

Table 2.1 Elements of Jacobian matrices in fast decoupled method.

Jacobian matrix	Diagonal element	Off-diagonal element
$[J_{P\theta}']$	$\frac{\partial P'_i}{\partial \theta_i} = \sum_k \frac{1}{k\epsilon a_i x_{ik}}$	$\frac{\partial P'_i}{\partial \theta_k} = \frac{1}{x_{ik}}$
$[J_{QV}']$	$\frac{\partial Q'_i}{\partial v_i} = -\sum_k \left( \frac{1}{k\epsilon a_i x_{ik}} + s_{ik} \right)$	$\frac{\partial Q'_i}{\partial v_k} = \frac{1}{x_{ik}}$

In Table 2.1 the superscript prime (') implies reformulation of the equations (2.1) and (2.2) due to their division by the corresponding bus voltage magnitude.



Equation (2.7) and (2.8) can be rewritten for  $[\Delta\theta]$  and  $[\Delta v]$  as follows.

$$[\Delta\theta]^{m+1} = [J'_{P\theta}]^{-1} \left[ \frac{\Delta P}{V} \right]^{m+1} \quad (2.15)$$

$$[\Delta v]^{m+1} = [J'_{Qv}]^{-1} \left[ \frac{\Delta Q}{V} \right]^{m+1} \quad (2.16)$$

when

$$\left( \frac{\Delta P}{V} \right)_i^{m+1} = \frac{P_i}{V_i} - \frac{P_i(v^m, \theta^m)}{V_i} \quad (2.17)$$

$$\left( \frac{\Delta Q}{V} \right)_i^{m+1} = \frac{Q_i}{V_i} - \frac{Q_i(v^m, \theta^m)}{V_i} \quad (2.18)$$

A flow chart of the fast decoupled algorithm for integrated load flow analysis of a system is shown in Figure 2.1.

### 2.3 Bifactorisation of Sparse Jacobian Matrices

A power system network has a sparse topology i.e. on the average one or two branches is connected to a bus so that the symmetrical Jacobian matrices  $[J'_{P\theta}]$  in equations (2.15) and  $[J'_{Qv}]$  in equation (2.16) are also sparse i.e. with a great number of zeros in off-diagonal positions. Hence significant savings in storage and computation time can be achieved by storing and operating upon only the non-zero elements during inversions of the

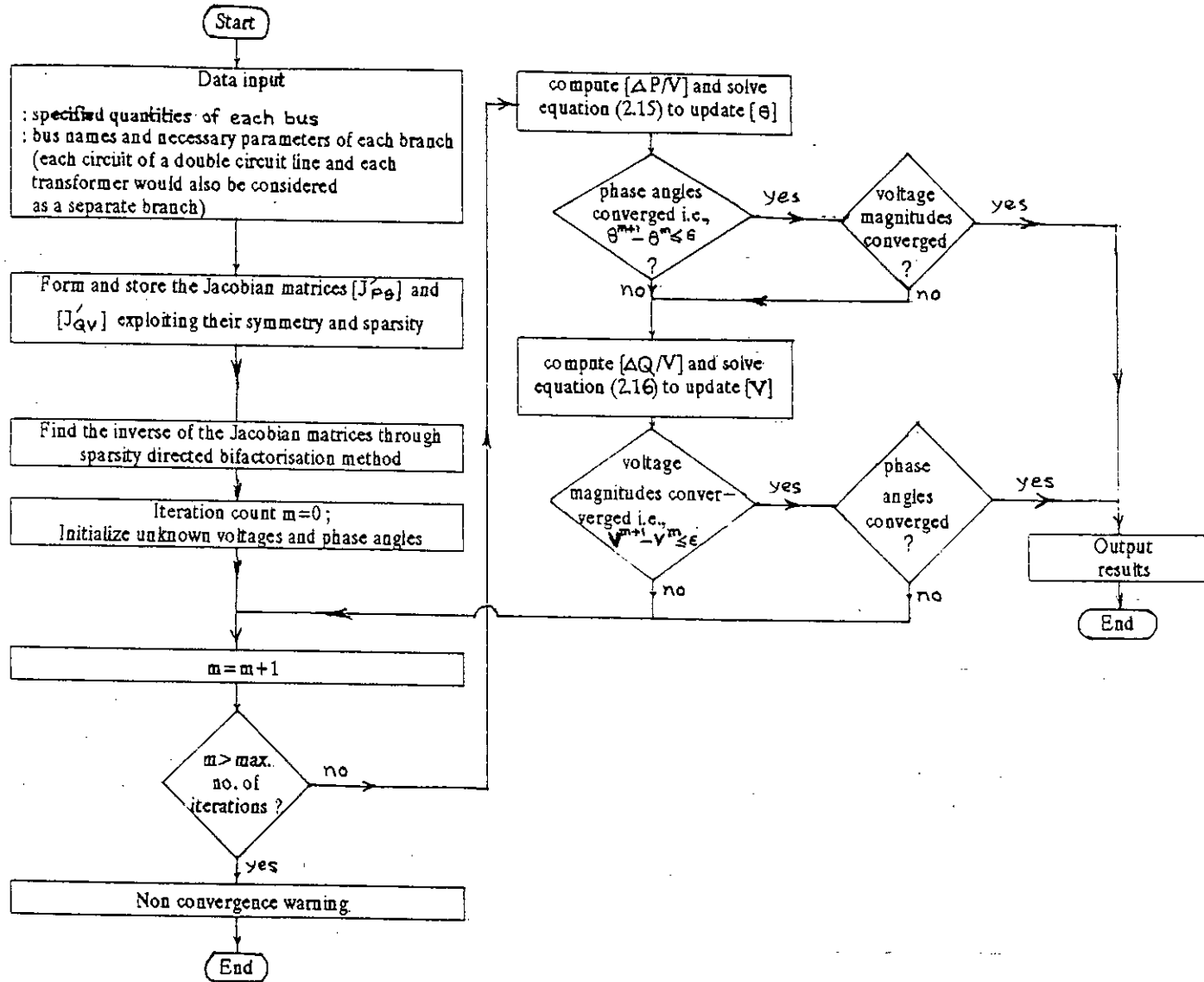


Figure 2.1 Flow chart for the fast decoupled algorithm in integrated mode

Jacobian matrices. For this, a technique known as bifactorisation method<sup>3</sup> is used instead of explicit inversion through Gauss Jordan elimination or some other conventional method.

The process of inversion through sparsity directed bifactorisation of a symmetrical Jacobian matrix can conveniently be divided<sup>3</sup> into four steps viz : i) storing, ii) ordering i.e. establishing the elimination sequence or selection of the pivotal columns, iii) reduction i.e. obtaining the  $2N$  number of factor matrices called left and right hand factors,  $N$  being the order of the Jacobian matrix and iv) solution i.e. multiplying the right side known vector  $[\Delta P/v]$  or  $[\Delta Q/v]$  by the  $2N$  factor matrices one after another so that at the end  $[\Delta P/v]$  or  $[\Delta Q/v]$  become the solution vector  $[\Delta \theta]$  or  $[\Delta v]$ .

The factor matrices are such that for a symmetrical matrix the left and right hand factors of the same order i.e.  $[L^k]$  and  $[R^k]$  have the same off-diagonal non-zero elements excepting the diagonal element which is nonunity for the left hand factor while unity for the right hand factor. Moreover, the non-zero off-diagonal elements are only in the  $k$ -th column and below the diagonal element of the  $k$ -th left hand factor while only in the  $k$ -th row and right to the

diagonal element of the k-th right hand factor. So it is sufficient to determine and store only the non-zero elements of a single column i.e. the k-th column of each left hand factor matrix  $[L^k]$ .

The storing of the non-zero elements is done using a one dimensional array while the indexing for their identification and retrieval is done using only five more integer type arrays of same or shorter size.

#### 2.4 Conclusions

In the fast decoupled method the nonlinear load flow analysis is divided into two subproblems viz : active power-phase angle (P- $\theta$ ) and reactive power-voltage magnitude (Q-V) problems neglecting the weak coupling of P-V and Q- $\theta$  quantities. But in each iteration the two subproblems are solved with constant Jacobian matrices which need to be involved only once outside the iterative loop. However, to save further CPU time and memory this inversion is done using the sparsity directed bifactorisation method instead of the inefficient conventional methods which makes a sparse matrix full after its explicit inversion.

In the integrated approach the active and reactive Jacobian matrices are formed considering the whole system as a single piece. Though sparsity is exploited the CPU time and storage requirement for a large system may still be high unless the fast decoupled method is considered together with decomposition of the system into a number of subsystem.

**CHAPTER 3**  
**DECOMPOSED LOAD FLOW ANALYSIS**  
**THROUGH SPACE DECOUPLING**

### 3.1 Introduction

The dimensions of the active and reactive Jacobian matrices of the most efficient integrated load flow method i.e. the fast decoupled technique increase with the size (number of buses) of a power system so that even sparsity exploitation in those matrices may not be enough to achieve on-line computability. This necessitates system decomposition. As mentioned in Chapter 1 the existing decomposed load flow analysis algorithms are mainly based on separate solution of the model comprising the tie lines between subsystems and also the temporary fictitious slack buses in subsystems (for some of the algorithms). In the present research project an investigation has been made for combining the tie lines in subsystem models.

### 3.2 Proposed Technique of Space Decoupling

The underlying principle of the proposed decomposed load flow analysis can best be illustrated through an example. Let a system be divided into two subsystems as in Figure 3.1.

Then the active Jacobian matrix for using the fast decoupled algorithm in the considered system will have the structure shown in Figure 3.2.

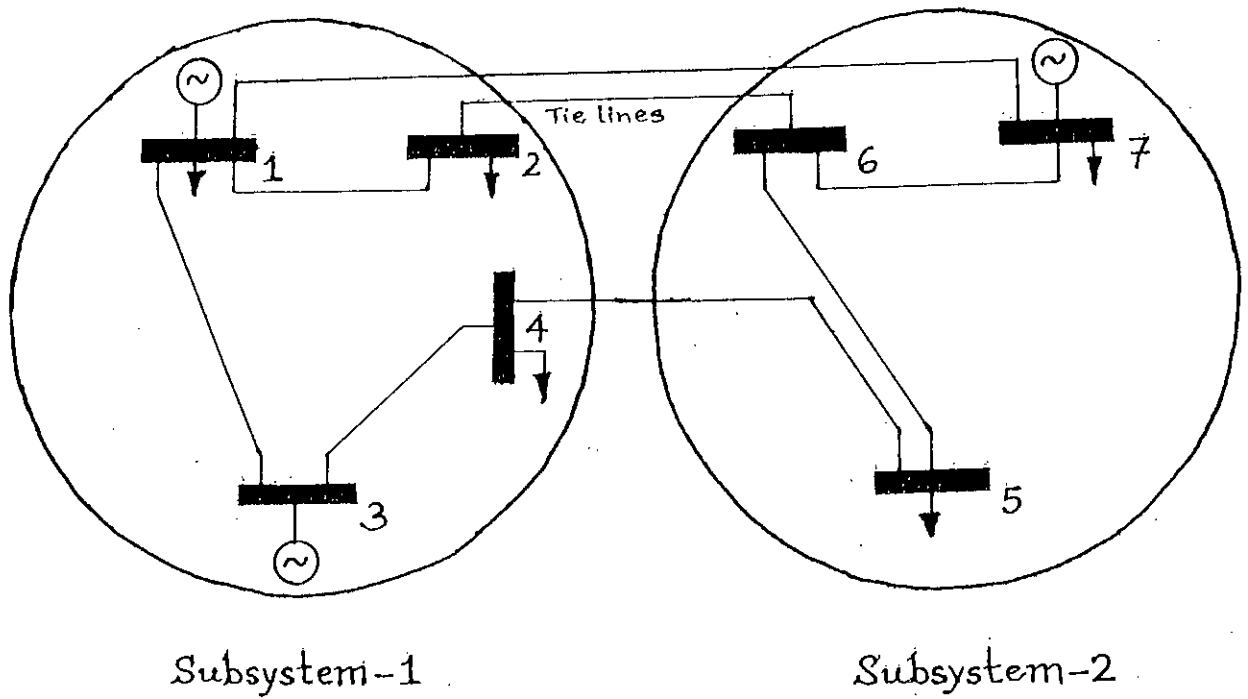


Figure 3.1 Decomposition of a system into two subsystems

	1	2	3	4	5	6	7
1	$\begin{bmatrix} \frac{\partial P}{\partial \theta} \end{bmatrix}_{11}$				$\begin{bmatrix} \frac{\partial P}{\partial \theta} \end{bmatrix}_{12}$		
2							
3							
4							
5	$\begin{bmatrix} \frac{\partial P}{\partial \theta} \end{bmatrix}_{21}$				$\begin{bmatrix} \frac{\partial P}{\partial \theta} \end{bmatrix}_{22}$		
6							
7							

Figure 3.2 Structure of active Jacobian matrix



In Figure 3.2 the subscript 11 refers to the derivatives of active powers in subsystem-1 with respect to the phase angles of the nodes only in the same subsystem while 12 refers to the derivatives of active powers in subsystem-1 with respect to the phase angles of the nodes in subsystem-2. Similar significance holds good for the subscript 21 and 22.

In the proposed technique the off-diagonal blocks  $[\frac{\partial P}{\partial \theta}]_{12}$  and  $[\frac{\partial P}{\partial \theta}]_{21}$  representing the coupling of subsystems 1 and 2 through the tie lines are not considered so that the Jacobian structure is as in Figure 3.3.

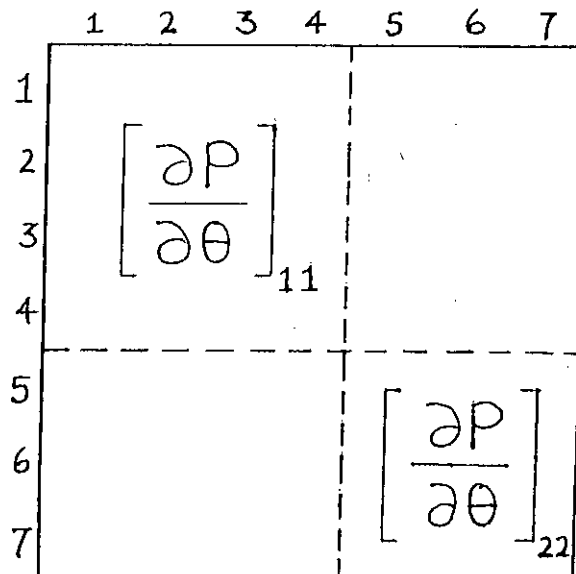


Figure 3.3 Structure of the space decoupled Jacobian matrix

Since in Figure 3.3 the two subsystem Jacobian submatrices have been space decoupled the equation (2.15) for the phase angle solution can be written subsystemwise as follows.

$$[\Delta\theta]_1^{m+1} = [J'_{P\theta}]_{11}^{-1} \left[ \frac{\Delta P}{V} \right]_1^{m+1} \quad (3.1)$$

$$[\Delta\theta]_2^{m+1} = [J'_{P\theta}]_{22}^{-1} \left[ \frac{\Delta P}{V} \right]_2^{m+1} \quad (3.2)$$

In equations (3.1) and (3.2) subscripts 1 and 2 corresponds to subsystems 1 and 2 respectively. It should be noted that equations (3.1) and (3.2) can be solved simultaneously in respective subsystem in each iteration.

It is worthnoting that for the example shown the admittance of the tie line between nodes 1 (subsystem-1) and 7 (subsystem-2) has been included in the element  $\frac{\partial P_1}{\partial \theta_1}$  of the subsystem-1 Jacobian matrix  $[J_{P\theta}]_{11}$  i.e.  $[\frac{\partial P}{\partial \theta}]_{11}$  and in  $-\frac{\partial P_7}{\partial \theta_1}$  of the subsystem-2 Jacobian matrix  $[J_{P\theta}]_{22}$  i.e.  $[\frac{\partial P}{\partial \theta}]_{22}$ . Similarly the other tie lines 2-6 and 4-5 have been treated.

The proposed way of space decoupling and tie line modelling has an added advantage of overcoming singularity problem in the active Jacobian matrices of those subsystems which do not contain the system slack bus.

The example can easily be extended for a more generalized case of system decomposition with more than two subsystems.

Space decoupling has been introduced by the present method for reactive Jacobian matrix in a way similar to that shown for the active Jacobian matrix so that equation (2.16) for the voltage magnitudes solution can be written subsystemwise as follows.

$$[\Delta V]_i^{m+1} = [J'_{\theta v}]_{ii}^{-1} \left[ \frac{\Delta P}{V} \right]_i^{m+1} \quad (3.3)$$

where,

$i = 1, 2, \dots, \dots$  No. of subsystem.

$$\begin{bmatrix} \Delta\theta_1 \\ \Delta\theta_2 \\ \Delta\theta_3 \\ \Delta\theta_4 \\ \Delta\theta_5 \\ \Delta\theta_6 \\ \Delta\theta_7 \end{bmatrix}^{m+1} = \begin{bmatrix} 1 & 2 & 3 & 4 & 5 & 6 & 7 \\ \times & \times & \times & \times & \times & \times & \times \\ \times & \times & \times & \times & \times & \times & \times \\ \times & \times & \times & \times & \times & \times & \times \\ \times & \times & \times & \times & \times & \times & \times \\ \times & \times & \times & \times & \times & \times & \times \\ \times & \times & \times & \times & \times & \times & \times \end{bmatrix} \begin{bmatrix} 1 \\ 2 \\ 3 \\ 4 \\ 5 \\ 6 \\ 7 \end{bmatrix} \begin{bmatrix} \times \\ \times \\ \times \\ \Delta P/V \\ \times \\ \times \\ \times \end{bmatrix}^{m+1}$$

$J'_{P\theta}$

Figure 3.4 Solution of the equation  $[\Delta\theta] = [J'_{P\theta}]^{-1} [\Delta P/V]$  for the system of Figure 3.1 in integrated manner

The effects of proposed space decoupling upon the solution quality can be illustrated with respect to the example system of Figure 3.1. When this system is solved in integrated manner using the fast decoupled method, the solution for phase angles become as in Figure 3.4.

It is evident that due to the integrated approach the effects of  $[\Delta P/V]$  elements corresponding to the nodes 5, 6, 7 in the subsystem-2 also spread to phase angle solution of each node in subsystem-1 through the product  $[J_{p\theta}]^{-1} [\Delta P/V]$ , though all of them

$$\begin{bmatrix} \Delta\theta_1 \\ \Delta\theta_2 \\ \Delta\theta_3 \\ \Delta\theta_4 \\ \hline \Delta\theta_5 \\ \Delta\theta_6 \\ \Delta\theta_7 \end{bmatrix}^{m+1} = \begin{bmatrix} 1 & 2 & 3 & 4 & 5 & 6 & 7 \\ \times & \times & \times & \times & & & \\ \times & \times & J_{P\theta_{11}}^{-1} & \times & & & \\ \times & \times & & \times & & & \\ \times & \times & \times & \times & & & \\ \hline & & & & \times & \times & \times \\ & & & & \times & J_{P\theta_{22}}^{-1} & \times \\ & & & & \times & \times & \times \end{bmatrix} \begin{bmatrix} 1 \\ 2 \\ 3 \\ 4 \\ \hline 5 \\ 6 \\ 7 \end{bmatrix} \begin{bmatrix} \times \\ \frac{\Delta x_p}{V_1} \\ \times \\ \times \\ \hline \times \\ \frac{\Delta P}{V_2} \\ \times \end{bmatrix}^{m+1}$$

Figure 3.5 Solution of the equations (3.1) and (3.2) for the system of Figure 3.1 in the space decoupled method

are not connected through tie lines to the nodes in subsystem-2. Similarly the effects of subsystem-1 elements in  $[\Delta P/V]$  spread to subsystem-2. It should be noted that  $[J_{pg}']^{-1}$  has been shown as explicit inverse in Figure 3.4 for the ease in understanding. Otherwise  $[J_{pg}']^{-1}$  is always stored as 2N factor matrices in the bifactorisation method and the multiplication  $[J_{pg}']^{-1} [\Delta P/V]^{n+1}$  is done through these factors as and when needed.

Now when the system of Figure 3.1 is solved piecewise through space decoupling using equations (3.1) and (3.2) the solution for phase angles become as in Figure 3.5.

It is evident that though the injection vectors  $[\frac{\Delta P}{V}]_1$  and  $[\frac{\Delta P}{V}]_2$  of the subsystem-1 and subsystem-2 respectively are the same as the corresponding pairs in  $[\Delta P/V]$  of Figure 3.4 for the integrated method, the effects of one subsystem elements in the injection vector do not spread to the other subsystem's phase angle solutions through multiplication by the space decoupled Jacobian matrix. The effects of this non-spreading depends upon the magnitude of tie line impedances and would more affect the boundary nodes in the two subsystems than their other nodes. However this dependence would always be nonlinear and among other things would also depend upon the number of boundary nodes, the total number of nodes, the number of tie lines and self lines and the difference between local generation and demand in a subsystem. The term 'self' implies those lines only within a subsystem.

The foregoing comments on effects of non-spreading of each node's injection to the other nodes also hold good for voltage magnitude solution by the proposed space decoupled load flow technique.

### 3.3 Flow Chart for the Proposed Decomposed Load Flow Analysis

A flow chart for the fast decoupled algorithm for the proposed decomposed load flow analysis is shown in Figure 3.6.

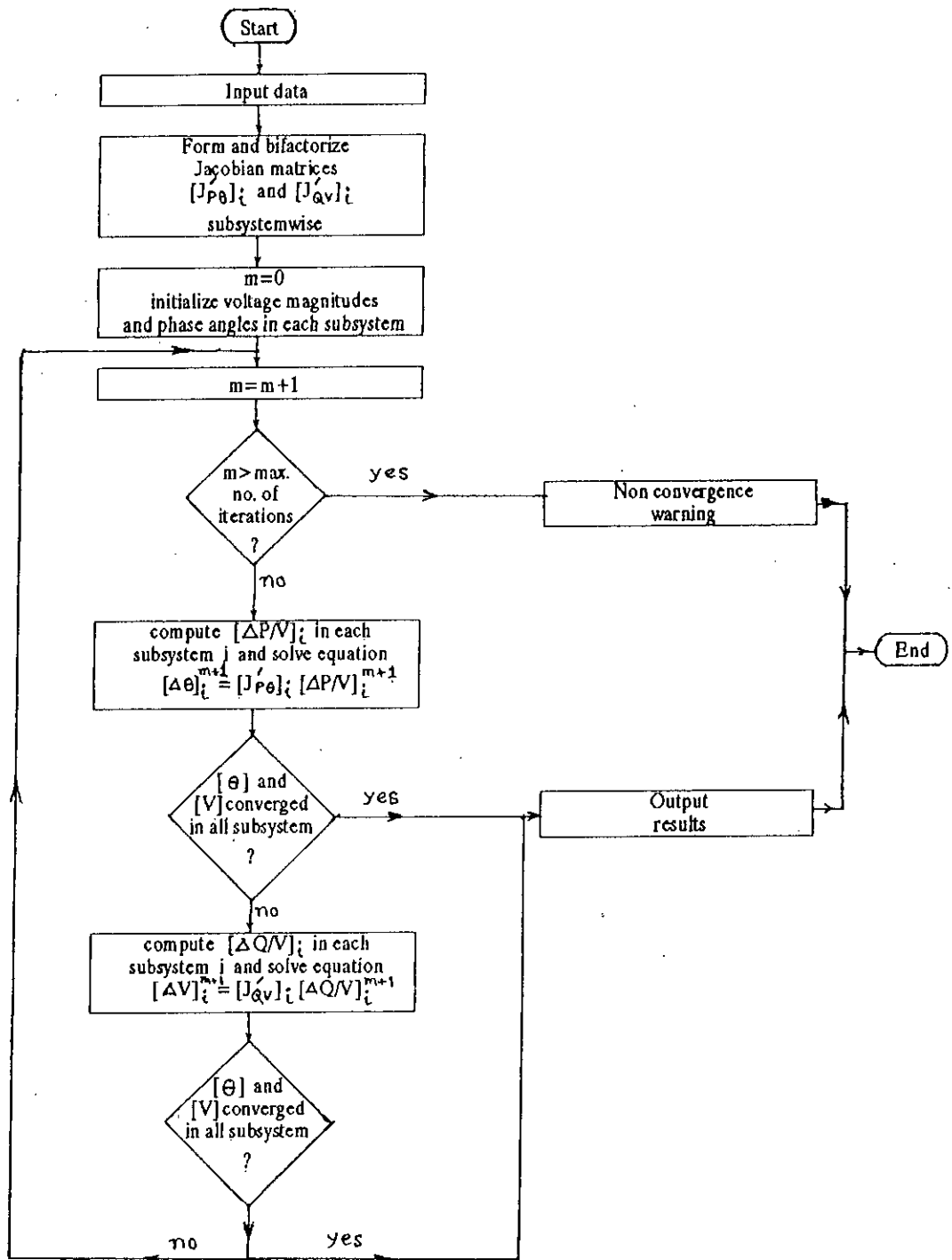


Figure 3.6 Flow chart for the fast decomposed algorithm in decomposed mode.

### 3.4 Conclusions

A decomposed load flow analysis method has been proposed in which active and reactive Jacobian matrices would be formed for each subsystem including the tie lines only in the diagonal elements and neglecting the off-diagonal elements representing the coupling between the subsystems. However, the injection vector of each subsystem will be formed considering the tie line flows. The proposed technique will enable load flow solution of a system of any size parallelly in a number of subsystems without any singularity problem and without requiring separate tie line model solution. The effect of proposed space decoupling in the Jacobian matrices is expected to be nonlinearly dependent upon the number of boundary nodes, the total number of nodes, the number of tie lines and self lines and the difference between specified local generation and demand in a subsystem etc.



**CHAPTER 4**  
**PRESENTATION OF RESULTS**

#### 4.1 Introduction

The proposed space decoupled load flow technique also referred to as the decomposed load flow analysis was tested and compared extensively against the integrated approach on four systems of diverse size and characteristics. These are IEEE 14 bus, 30 bus, 57 bus and a practical 81 bus system i.e. Bangladesh Power Development Board (BPDB) grid network. The test systems were divided quite arbitrarily into a number of subsystems to investigate into the performance of the decomposed method. Also both the methods were tested changing the operating conditions of the four systems in various ways. Both the methods used fast decoupling and sparsity exploitation techniques. The performance of the two methods have been compared using two main criteria viz : mismatch and number of iterations required for convergence. Mismatch at a node is the difference between specified and calculated injection (active / reactive). The acceptable<sup>2</sup> upper limit of active and reactive power mismatch at any mode is on the average 1 MW or MVAR. The convergence was checked using a tolerance margin of 0.001 i.e. the change in voltage magnitude and phase angle at each bus between two consecutive iterations should be less than or equal to 0.001 for convergence. The iterative scheme was started for both the methods with flat values i.e.  $1.0\angle 0^\circ$  per unit for unknown voltage

magnitudes and phase angles of the buses. The computational performance was compared in terms of CPU time and core memory requirements. Both the methods were programmed in FORTRAN 77 and run on IBM 4331/KO2 mainframe computer.

#### 4.2 Study of IEEE 14 Bus System

A single line diagram of the system is shown in Figure 4.1. The bus and line data are given in Appendix A. Two cases were studied by the decomposed load flow method. Though in both the cases the number of subsystems was two they differed from each other in the operating conditions. For the two cases the integrated load flow analysis was conducted considering the system in a single piece. The particulars of the two cases and the results obtained from the two methods have been shown in Table 4.1.

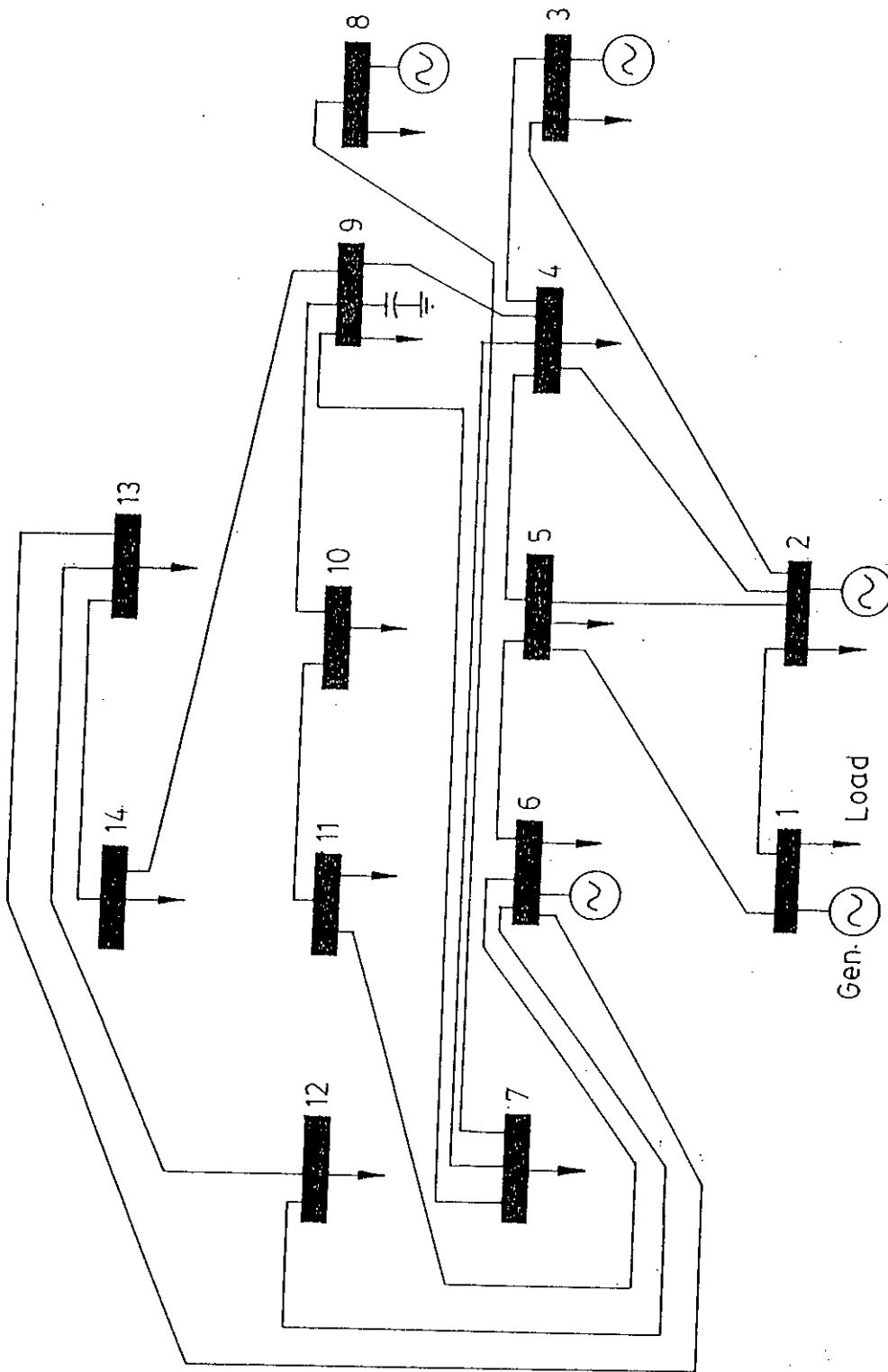


Figure 4.1 Single line diagram of the IEEE 14 bus system

Table 4.1 : Comparison of decomposed and integrated load flow analyses of the IEEE 14 bus system

Case No.	Total no. of PV buses	Total specified load	Total specified active power generation excluding slack generation	Decomposed method				Integrated method		
				Subsystem particulars	Slack bus generation (MW/MVAR)	Average mismatch at each node (MW/MVAR)	No. of iterations	Slack bus generation (MW/MVAR)	Average mismatch at each node (MW/MVAR)	No. of iterations
I	4	258.3 MW	40.0 MW	SS-1 : $P_1 = 66.05\%$ , $N_1 = 5$ , $N_2 = 2$ $P_2 = 100\%$ , $N_3 = 3$ , $N_4 = 2$	220.5 MW	-0.111 MW	17	252.3 MW	-0.007 MW	11
		81.3 MVAR		SS-2 : $P_1 = 33.95\%$ , $N_1 = 9$ , $N_2 = 3$ $P_2 = 0\%$ , $N_3 = 3$ , $N_4 = 2$	-21.9 MVAR	-0.01 MVAR		-22.0 MVAR	0.0 MVAR	
II	6	258.3 MW	308.0 MW	SS-1 : $P_1 = 66.05\%$ , $N_1 = 5$ , $N_2 = 2$ $P_2 = 64.93\%$ , $N_3 = 3$ , $N_4 = 2$	-40.3 MW	0.108 MW	9	-41.9 MW	-0.005 MW	7
		81.3 MVAR		SS-2 : $P_1 = 33.95\%$ , $N_1 = 9$ , $N_2 = 3$ $P_2 = 35.07\%$ , $N_3 = 3$ , $N_4 = 4$	42.2 MVAR	0.006 MVAR		42.6 MVAR	0.0 MVAR	

SS : subsystem

$N_1$  : No. of nodes in the subsystem

$N_3$  : No. of tie lines in the subsystem

$P_1$  : Percentage of specified active power generation in the subsystem

$N_2$  : No. of boundary nodes in the subsystem

$N_4$  : No. of PV buses in the subsystem

$P_2$  : Percentage of specified active load in the subsystem

In case I reported in Table 4.1, out of the generators at four buses (node nos. 2, 3, 6 and 8) only the generator at node 2 was committed in addition to the slack (node no. 1) generator. For the decomposed load flow analysis in case I, the system was divided into two subsystems removing three lines respectively 5-6, 4-7 and 4-9 such that the buses 1 to 5 were in subsystem-1 while 6 to 14 were in subsystem-2. Consequently the 100% of the committed active power generation was in subsystem-1 resulting in an unbalance between local demand (active load) and generation for subsystem-2. This made the decomposed load flow algorithm converge in 17 iterations i.e. 6 iterations more than that required by the integrated method for case I.

In case II bus nos. 11 and 14 were also assumed as PV buses in addition to those in case I. Also more generators e.g. at bus nos. 2, 3, 6, 8 and 11 were committed for active power while the load remained the same in case I. For the decomposed method though the subsystems' configurations (total no. of nodes, tie lines, boundary nodes) are the same as in case I, case II has resulted in a more uniformity in the balance between local demand and generation in each subsystem and hence an improvement in the convergence over case I. Case II required only 9 iterations for the decomposed

method which is just 2 iterations more than that of the integrated load flow analysis of case II.

A comparison of the mismatches obtained in the two methods shows that the average mismatch per node is in acceptable range. However, the MVAR mismatch in the decomposed load flow analysis was less and closer to that of the integrated analysis compared to the MW mismatch. This reflects the fact that in the two methods the obtained voltage magnitudes were almost identical while the phase angles differed by a maximum of 0.1 degree. One of the reasons of less reactive power mismatch is that the unknown voltage magnitudes are initially chosen as 1.0 p.u. nearing the finally achievable values. On the otherhand the phase angles are set at zero initial values as their final values can not be predicted in advance so that it is the active part solution which affects the decomposed method more than the integrated method and requires more iterations and hence produces more mismatch in active power.

### 4.3 Study of IEEE 30 Bus System

A single line diagram of the system is shown in Figure 4.2. The bus and line data are given in Appendix B. Three cases were studied by the decomposed load flow method. The first two cases have same operating conditions but differ only in the way the system was divided into two subsystems.

In the case I the two subsystems had 4 tie lines between them such that buses 1 to 25 were in subsystem-1 and 26 to 30 were in subsystem-2. The tie lines were respectively between buses 6-28, 8-28, 25-26 and 25-27.

In the case II the subsystem-1 comprised 24 buses (nos. 1 to 12, 14 to 25) and subsystem-2 comprised 6 buses (nos. 13, 26 to 30). There were 5 tie lines between the two subsystems respectively between buses 6-28, 8-28, 12-13, 25-26 and 25-27.

The case III differs from case I and II in the amount of specified active power generation and number of subsystems though the total load remained the same and the number of generator connected buses was 14 consisting of 13 PV buses and one slack bus (node no. 1) in all the three cases. In the case III the system was



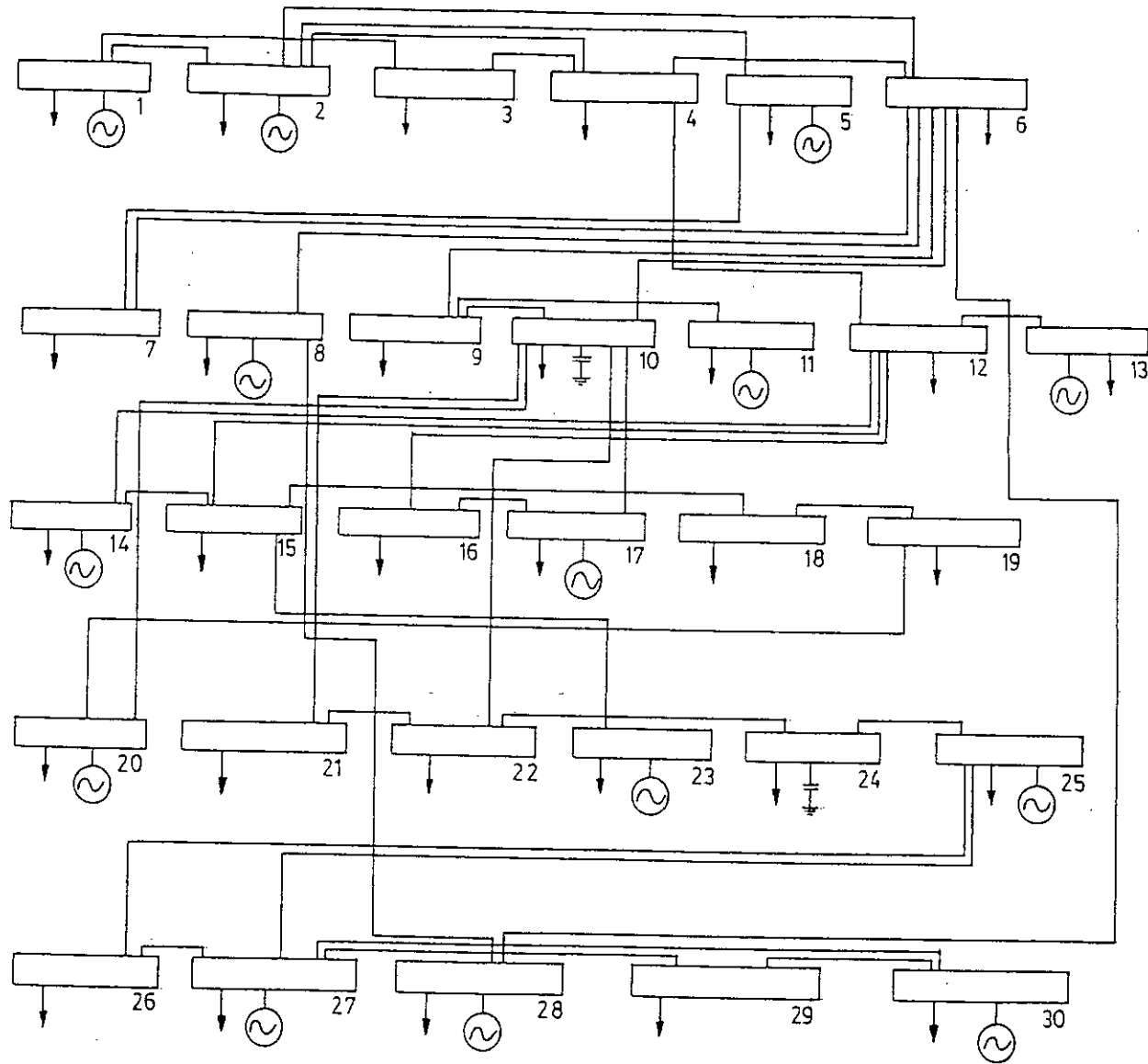


Figure 4.2 Single line diagram of the IEEE 30 bus system

divided into three subsystems. The subsystem-1 comprised 12 buses (nos. 1 to 6 and 14 to 19) and had 13 tie lines with subsystem-2 and subsystem-3. The subsystem-2 had also 12 buses (nos. 7 to 12 and 20 to 25) and 16 tie lines with subsystem-1 and subsystem-3. The subsystem-3 possessed 6 buses (nos. 13 and 26 to 30) and 5 tie lines with subsystem-1 and subsystem-2.

The cases I and III were also studied considering the 30 bus system in a single piece by the integrated load flow method for comparing with the results of the decomposed method. It is worthnoting that case I and case II are the same for the integrated method as the system is to be considered without its division into subsystems.

Table 4.2 shows the results obtained in the two methods of load flow analysis.

An analysis of the three cases reported in Table 4.2 shows that as regards the local balance between generation and demand, the system decomposition in case I was more uniform than the other two cases so that it took 17 iterations to converge. The case II with moderate uniformity in subsystemwise balance between

Table 4.2 : Comparison of decomposed and integrated load flow analyses of the IEEE 30 bus system

Case No.	Total specified Load	Total specified active power generation excluding slack generation	Decomposed method				Integrated method		
			Subsystem particulars	Slack bus generation (MW/MVAR)	Average mismatch at each node (MW/MVAR)	No. of iterations	Slack bus generation (MW/MVAR)	Average mismatch at each node (MW/MVAR)	No. of iterations
I	283.4 MW 126.2 MVAR	246.3 MW	SS-1 : $P_1 = 94.17\%$ , $N_1 = 25$ , $N_2 = 3$ $P_2 = 89.7\%$ , $N_3 = 4$ , $N_4 = 10$	42.1 MW	0.035 MW	17	41.1 MW	-0.001 MW	4
			SS-2 : $P_1 = 5.83\%$ , $N_1 = 5$ , $N_2 = 3$ $P_2 = 10.3\%$ , $N_3 = 4$ , $N_4 = 3$	21.8 MVAR	0.0 MVAR		22.1 MVAR	0.0 MVAR	
II	283.4 MW 126.2 MVAR	246.3 MW	SS-1 : $P_1 = 94.17\%$ , $N_1 = 24$ , $N_2 = 4$ $P_2 = 82.83\%$ , $N_3 = 5$ , $N_4 = 9$	42.2 MW	0.038 MW	19	Same as case I		
			SS-2 : $P_1 = 5.83\%$ , $N_1 = 6$ , $N_2 = 4$ $P_2 = 17.17\%$ , $N_3 = 5$ , $N_4 = 4$	41.8 MVAR	-0.0013 MVAR				
III	283.4 MW 126.2 MVAR	281.0 MW	SS-1 : $P_1 = 58.59\%$ , $N_1 = 12$ , $N_2 = 8$ $P_2 = 43.45\%$ , $N_3 = 13$ , $N_4 = 4$	8.9 MW	0.092 MW	52	6.1 MW	-0.001 MW	4
			SS-2 : $P_1 = 35.77\%$ , $N_1 = 12$ , $N_2 = 8$ $P_2 = 35.92\%$ , $N_3 = 16$ , $N_4 = 5$	31.3 MVAR	0.001 MVAR		32.0 MVAR	0.0 MVAR	
			SS-3 : $P_1 = 5.84\%$ , $N_1 = 6$ , $N_2 = 4$ $P_2 = 20.63\%$ , $N_3 = 5$ , $N_4 = 4$						

SS : subsystem

$N_1$  : No. of nodes in the subsystem

$N_3$  : No. of tie lines in the subsystem

$P_1$  : Percentage of specified active power generation in the subsystem

$N_2$  : No. of boundary nodes in the subsystem

$N_4$  : No. of PV buses in the subsystem

$P_2$  : Percentage of specified active load in the subsystem

generation and demand, required slightly more i.e. 19 iterations. The case III with three subsystems but a highly nonuniform balance between generation and demand in subsystem nos. 1 and 3 required 52 iterations. In all these three cases the integrated method took 4 iterations.

A lower mismatch in the integrated method reflects the fact that though this method has the drawback of dimensionality it has an advantage of solving the system in a single piece without requiring local uniformity between demand and generation to that extent as needed by the decomposed method. However, the mismatches in the decomposed method are also in the acceptable range for all the three cases.

It should be noted that in each of the three cases, the way the 30 bus system was divided into subsystems for the decomposed load flow analysis gave rise to few isolated nodes in some subsystems. These nodes had no connection with the remaining nodes of their own subsystem rather they had connections through tie lines with nodes of other subsystem(s). It is the topology of the 30 bus system that caused node isolation due to system decomposition. However, the proposed decomposed load flow analysis

technique has been successful in handling the node isolation problem and producing a converged solution. This success stems from the fact that each subsystem's injection vector considers the tie line flows though its Jacobian matrix does not contain any off-diagonal element corresponding to the tie lines.

#### 4.4 Study of IEEE 57 Bus System

A single line diagram of the system is shown in Figure 4.3. The bus and line data are given in Appendix C. Two cases were studied by both the decomposed and the integrated load flow methods. These two cases differ from each other in specified active power generation at PV buses. However, for the decomposed method the system was divided into two and three subsystems respectively in the case I and case II.

In the case I the two subsystems had 12 tie lines between them such that buses 1 to 16 were in subsystem-1 and 17 to 57 in subsystem-2. The number of boundary nodes in each subsystem was 10. In subsystem-1 the boundary nodes were respectively the bus nos. 1, 4, 7, 9, 10, 11, 12, 13, 14 and 15. The boundary nodes in subsystem-2 were respectively the bus nos. 17, 18, 29, 41, 43, 45, 46, 49, 51 and 55.

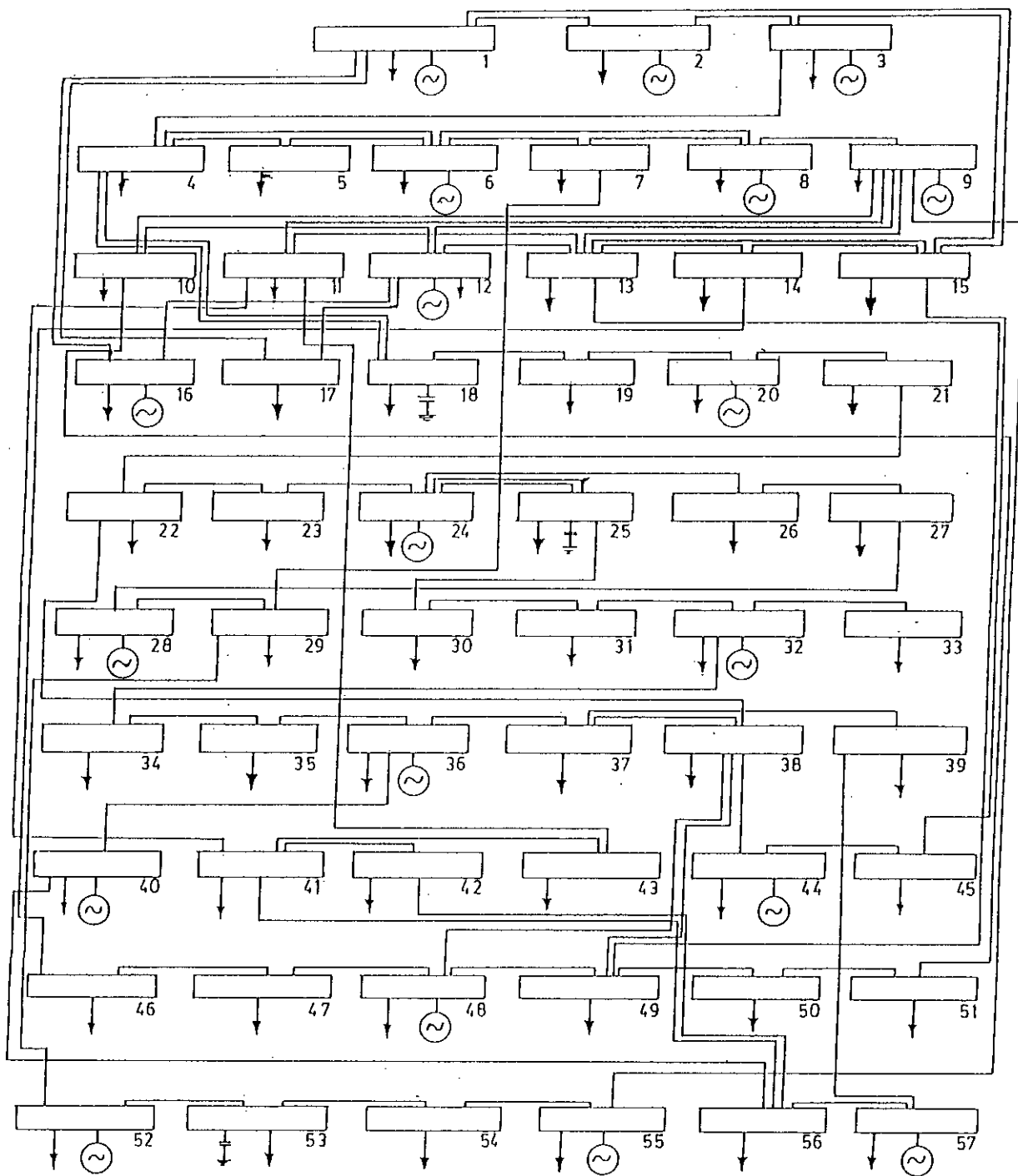


Figure 4.3 Single line diagram of the IEEE 57 bus system

In case II the number of nodes in the three subsystems were respectively 10, 30 and 17. The subsystem-1 comprised bus nos. 1 to 10 and it had 13 tie lines. The subsystem-2 comprised bus nos. 11 to 40 and it had 22 tie lines. The subsystem-3 included the bus nos. 41 to 57 and it had tie 13 tie lines.

In both the cases the number of generator connected buses was 19 consisting of 18 PV buses and one slack bus (node no. 1). Also the total load was same in the two cases.

Table 4.3 shows the results obtained by the two methods of load flow analysis for the two cases.

It is seen in Table 4.3 that for the decomposed method though the case I has two subsystems it converged in 11 iterations more than the case II with three subsystems. Because case I was more nonuniform regarding subsystemwise balance between active power generation and demand. The subsystem-1 of case I has an active load 24.46% more than its specified active generation and it amounts to on the average an imbalance of 1.52% per node as there are 16 nodes in this subsystem. On the otherhand, only the subsystem-2 of case II has a deficit of generation i.e. its active load is 29.9% more

Table 4.3 : Comparison of decomposed and integrated load flow analyses of the IEEE 57 bus system

Case No.	Total specified Load	Total specified active power generation excluding slack generation	Decomposed method				Integrated method		
			Subsystem particulars	Slack bus generation (MW/MVAR)	Average mismatch at each node (MW/MVAR)	No. of iterations	Slack bus generation (MW/MVAR)	Average mismatch at each node (MW/MVAR)	No. of iterations
I	1250.8 MW 336.0 MVAR	1120.0 MW	SS-1: $P_1 = 74.64\%$ , $N_1 = 16$ , $N_2 = 10$ $P_2 = 66.96\%$ , $N_3 = 12$ , $N_4 = 7$	163.4 MW	-0.05 MW	37	166.5 MW	-0.001 MW	6
			SS-2: $P_1 = 25.36\%$ , $N_1 = 41$ , $N_2 = 10$ $P_2 = 33.04\%$ , $N_3 = 12$ , $N_4 = 11$	156.0 MVAR	-0.003 MVAR		155.5 MVAR	0.0 MVAR	
III	1250.8 MW 336.0 MVAR	1298.0 MW	SS-1: $P_1 = 37.03\%$ , $N_1 = 10$ , $N_2 = 6$ $P_2 = 42.98\%$ , $N_3 = 13$ , $N_4 = 5$	6.9 MW	0.34 MW	26	-12.6 MW	-0.0008 MW	5
			SS-2: $P_1 = 49.85\%$ , $N_1 = 30$ , $N_2 = 12$ $P_2 = 36.98\%$ , $N_3 = 22$ , $N_4 = 8$	199.8 MVAR	-0.003 MVAR		204.3 MVAR	0.0001 MVAR	
			SS-3: $P_1 = 13.12\%$ , $N_1 = 17$ , $N_2 = 12$ $P_2 = 20.04\%$ , $N_3 = 13$ , $N_4 = 5$						

SS : subsystem

$N_1$  : No. of nodes in the subsystem

$N_3$  : No. of tie lines in the subsystem

$P_1$  : Percentage of specified active power generation in the subsystem

$N_2$  : No. of boundary nodes in the subsystem

$N_4$  : No. of PV buses in the subsystem

$P_2$  : Percentage of specified active load in the subsystem



than its specified active power generation and it amounts to on the average an imbalance of about 1% per node as there are 30 nodes in this subsystem. So among other factors it is also the average deficit per node in the amount of specified active power generation of a subsystem that affects the rate of convergence of the decomposed load flow analysis.

Requirement of a much less number of iterations for convergence of the integrated method stems from its advantage of considering the whole system in a single piece.

The average mismatch per node was acceptable in both the methods. However, the difference in the active power mismatch of the two methods was more than the difference in their reactive power mismatches. Apart from the reason mentioned for the 14 bus system in section 4.2, it is also due to the fact that in any load flow analysis method active power generation is calculated as output only for one bus i.e. the slack bus while required to be specified at all the remaining buses whereas the reactive power generation is calculated as output for a number of buses viz: all the PV buses and the slack bus. As mismatch is the difference between specified and calculated values of active or reactive power

the active power mismatch is zero only at slack bus while the reactive power mismatch is zero at a number of buses.

Like the 30 bus system, the decomposed load flow analysis of the 57 bus system was also successful in handling isolated nodes in each case. In the case I the subsystem-2 had 1 isolated node whereas in the case II the subsystem-2 and subsystem-3 had respectively 7 and 12 isolated nodes.

#### 4.5 Study of BPDB 81 Bus System

A single line diagram of the system is provided in Figure 4.4. The bus and line data are given in Appendix D.

The BPDB system is basically a 132 KV grid system with 25 major power stations with an installed capacity of about 2200 MW and a generation capability of about 1600 MW. It consists of two geographical zones viz: the East and the West, interconnected by a 230 KV double circuit transmission line. Due to the availability of natural gas major generation takes place in the East zone. The generation in the West zone depends upon imposed fuel. The total number of buses in the system is 81 including the slack bus (node no. 12) and 24 other generator connected PV buses. The total number

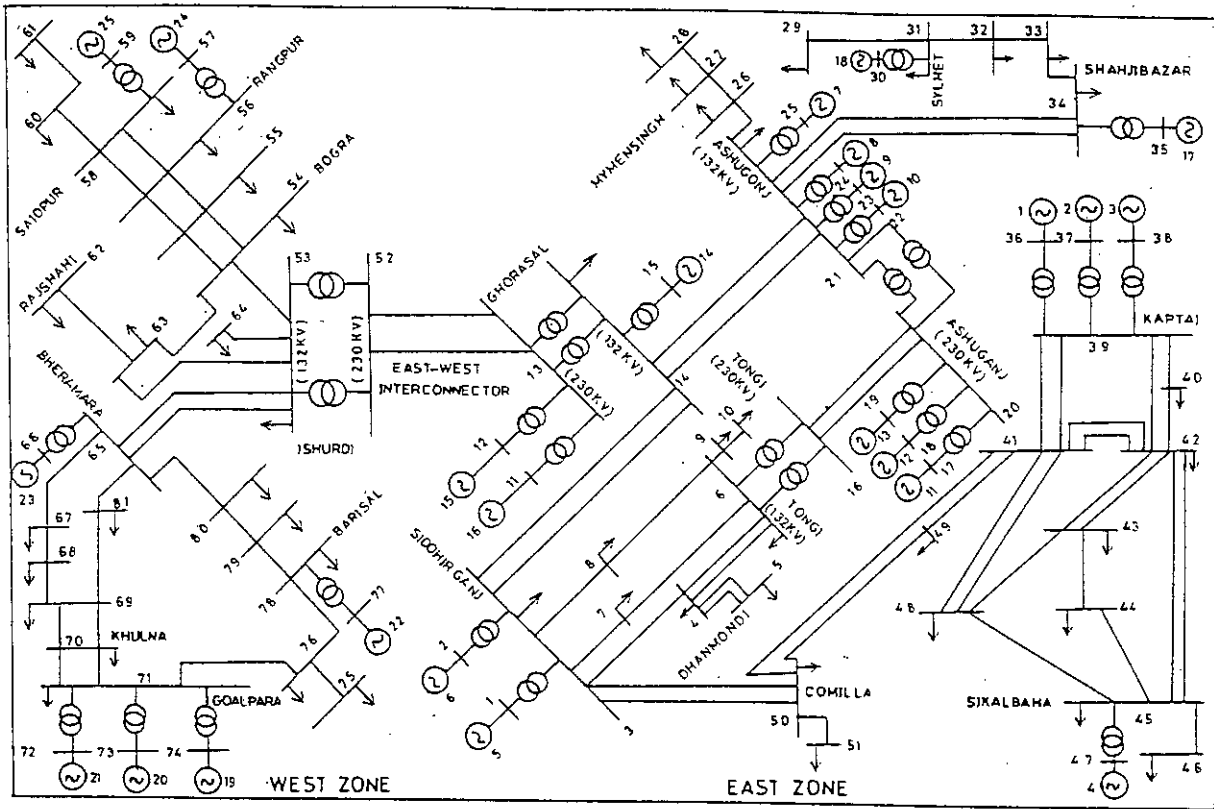


Figure 4.4 Single line diagram of the BPDB 81 bus system

of branches in the system is 114 consisting of the 132 KV and few 230 KV single or double circuit transmission lines, 25 step-up and 8 inter-bus (between 230 KV and 132 KV buses) transformers.

Three cases were studied by the decomposed and integrated methods of load flow analysis. The cases differ from each other in specified active power generation at PV buses. However, for the decomposed method, in both the cases I and II the system was divided into two subsystems i.e. the geographically existing East and West zones themselves. In the case III the system was divided into three subsystems of which two were obtained by further subdividing the East zone while the third subsystem comprised the West zone itself.

In both the cases I and II the two subsystems had 2 tie lines i.e. the double circuit East-West interconnector and only one boundary node each.

In the case III subsystems 1, 2 and 3 had respectively 4, 6 and 2 tie lines. The number of boundary nodes in them were respectively 2, 3 and 1.

Table 4.4 shows the results obtained by the two methods of load flow analysis for the three cases.

An analysis of the three cases reported in Table 4.4 reveals that in both cases I and II respectively having the highest and a moderate nonuniformity in subsystemwise balance between generation and demand, the decomposed load flow algorithm converged in 12 iterations which is 17 iterations less than that required by the same in the case III. This is due to the fact that though the case III has uniform active power balance its number of tie lines and boundary nodes was more than those in the cases I and II. Also there was no isolated node in any subsystem of the cases I and II. The rate of convergence of the decomposed algorithm also depends upon the number and location of tie lines, boundary nodes and isolated nodes in addition to the local uniformity in specified generation and demand.

It should be noted that though the subsystems' configurations were same and the decomposed method converged in same number of iterations in cases I and II, an improvement in the active power mismatch has resulted in the latter case due to its more uniformity in specified active power generation and demand than that

Table 4.4 : Comparison of decomposed and integrated load flow analyses of the BPDB 81 bus system

Case No.	Total specified Load	Total specified active power generation excluding slack generation	Decomposed method				Integrated method		
			Subsystem particulars	Slack bus generation (MW/MVAR)	Average mismatch at each node (MW/MVAR)	No. of iterations	Slack bus generation (MW/MVAR)	Average mismatch at each node (MW/MVAR)	No. of iterations
I	1427.3 MW 691.9 MVAR	1297.0 MW	SS-1: $P_1 = 70.55\%$ , $N_1 = 51$ , $N_2 = 1$ $P_2 = 92.1\%$ , $N_3 = 2$ , $N_4 = 17$	183.1 MW	-0.018 MW	12	184.6 MW	-0.0005 MW	7
			SS-2: $P_1 = 29.45\%$ , $N_1 = 30$ , $N_2 = 1$ $P_2 = 7.1\%$ , $N_3 = 2$ , $N_4 = 7$	70.3 MVAR	-0.001 MVAR		70.7 MVAR	0.0003 MVAR	
II	1427.3 MW 691.9 MVAR	1360.0 MW	SS-1: $P_1 = 70.55\%$ , $N_1 = 51$ , $N_2 = 1$ $P_2 = 75\%$ , $N_3 = 2$ , $N_4 = 7$	95.4 MW	0.023 MW	12	95.2 MW	0.0007 MW	4
			SS-2: $P_1 = 29.44\%$ , $N_1 = 30$ , $N_2 = 1$ $P_2 = 25\%$ , $N_3 = 2$ , $N_4 = 7$	40.6 MVAR	0.0034 MVAR		40.5 MVAR	0.0003 MVAR	
III	1427.3 MW 691.9 MVAR	1235.0 MW	SS-1: $P_1 = 20.1\%$ , $N_1 = 20$ , $N_2 = 2$ $P_2 = 23.1\%$ , $N_3 = 4$ , $N_4 = 6$	214.5 MW	-0.052 MW	29	218.9 MW	0.0 MW	4
			SS-2: $P_1 = 50.45\%$ , $N_1 = 31$ , $N_2 = 3$ $P_2 = 49.4\%$ , $N_3 = 6$ , $N_4 = 11$	48.8 MVAR	-0.0014 MVAR		49.3 MVAR	-0.0001 MVAR	
			SS-3: $P_1 = 29.45\%$ , $N_1 = 30$ , $N_2 = 1$ $P_2 = 27.5\%$ , $N_3 = 2$ , $N_4 = 7$						

SS : subsystem

$N_1$  : No. of nodes in the subsystem

$N_3$  : No. of tie lines in the subsystem

$P_1$  : Percentage of specified active power generation in the subsystem

$N_2$  : No. of boundary nodes in the subsystem

$N_4$  : No. of PV buses in the subsystem

$P_2$  : Percentage of specified active load in the subsystem

in case I. However, in all the cases the average mismatches were in acceptable range.

For the inherent advantage of treating the system in a single piece and hence spreading the effect of injection term at any node to the remaining nodes the integrated method involved less mismatch and less number of iterations in all the three cases.

It is worthnoting that the case III had 7 isolated nodes in the subsystem-1. However, the decomposed load flow algorithm handled it successfully in the way as explained for the cases of IEEE 30 and 57 bus systems in sections 4.3 and 4.4 respectively.

#### 4.6 Analysis of the Decomposed Method's

##### Convergence Characteristics

The results and discussions presented in sections 4.2 to 4.5 for various systems reveal that the main factors influencing the convergence of the decomposed load flow analysis are balance between specified active power generation ( $P_{sp.gen.}$ ) and load ( $P_{load}$ ), system size and the number of boundary nodes and tie lines. Also it was found that the difference between active power mismatches of the decomposed and the integrated methods was more than the

difference between their reactive power mismatches. So an 'at-a-glance-comparison' of the decomposed method's convergence characteristics as a function of the aforesaid main factors have been shown in Figures 4.5 and 4.6.

The number of iterations required by the decomposed and the integrated method with the variation of the specified active power balance has been shown in Table 4.5 and Figure 4.5 for various operating conditions of the four test systems. Since the decomposed method's convergence also depends upon the number of boundary nodes and tie lines these are also shown inside brackets at the points in Figure 4.5 corresponding to various cases of decomposing the system. As the integrated method does not require decomposing a system into subsystem the balance has been calculated as the difference between total specified active power generation and total specified active load i.e.  $(\sum P_{sp.gen.} - \sum P_{load})$ . To consider the system size the balance has been divided by the number of buses in the system.

It should be noted that in addition to those discussed in sections 4.2 to 4.5 few more cases with different operating conditions were also studied for both the methods. For the



decomposed method these cases considered different decomposition schemes. Table 4.5 also shows these cases.

It can be seen in Table 4.5 and Figure 4.5 that the integrated method converged in an approximately uniform way taking less number of iterations in all the cases of power balance whether they represent positive or negative balance i.e. deficit or surplus generation. This is due to its inherent feature of spreading the effect of injection at each bus to all other buses of the system. On the other hand the decomposed method required more iterations due to its confining the effect of injection at a bus only within the concerned subsystem. In general the number of iterations taken by decomposed method for a given system decreased so long there was

Table 4.5 : Summary of iterations vs. active power balance, number of tie lines and boundary nodes

System	Case	Average active power balance (MW/bus)	Integrated method	Decomposed method		
			ITER.	TBN	TNT	ITER.
14 Bus	I	-15.59	11	5	3	17
	II	3.55	7	5	3	9
	III	2.26	7	8	6	28
30 Bus	I	-1.23	4	6	4	17
	II	-1.23	4	8	5	19
	III	0.08	4	20	17	52
	IV	-4.38	4	15	12	N.C.(100)
	V	-4.38	4	8	5	N.C.(100)
	VI	-1.78	4	8	5	N.C.(100)
57 Bus	I	-2.29	6	20	12	37
	II	0.828	5	30	24	26
	III	-7.908	5	21	14	N.C.(100)
	IV	-2.82	5	21	11	N.C.(100)
BPDB	I	-1.608	7	2	2	12
	II	-0.8308	4	2	2	12
	III	-2.374	4	7	6	29
	IV	-1.20	6	6	6	N.C.(100)

ITER. : No. of iterations required for convergence

TBN : Total no. of boundary nodes

N.C.(100) : No convergence in 100 iterations

TNT : Total no. of tie lines

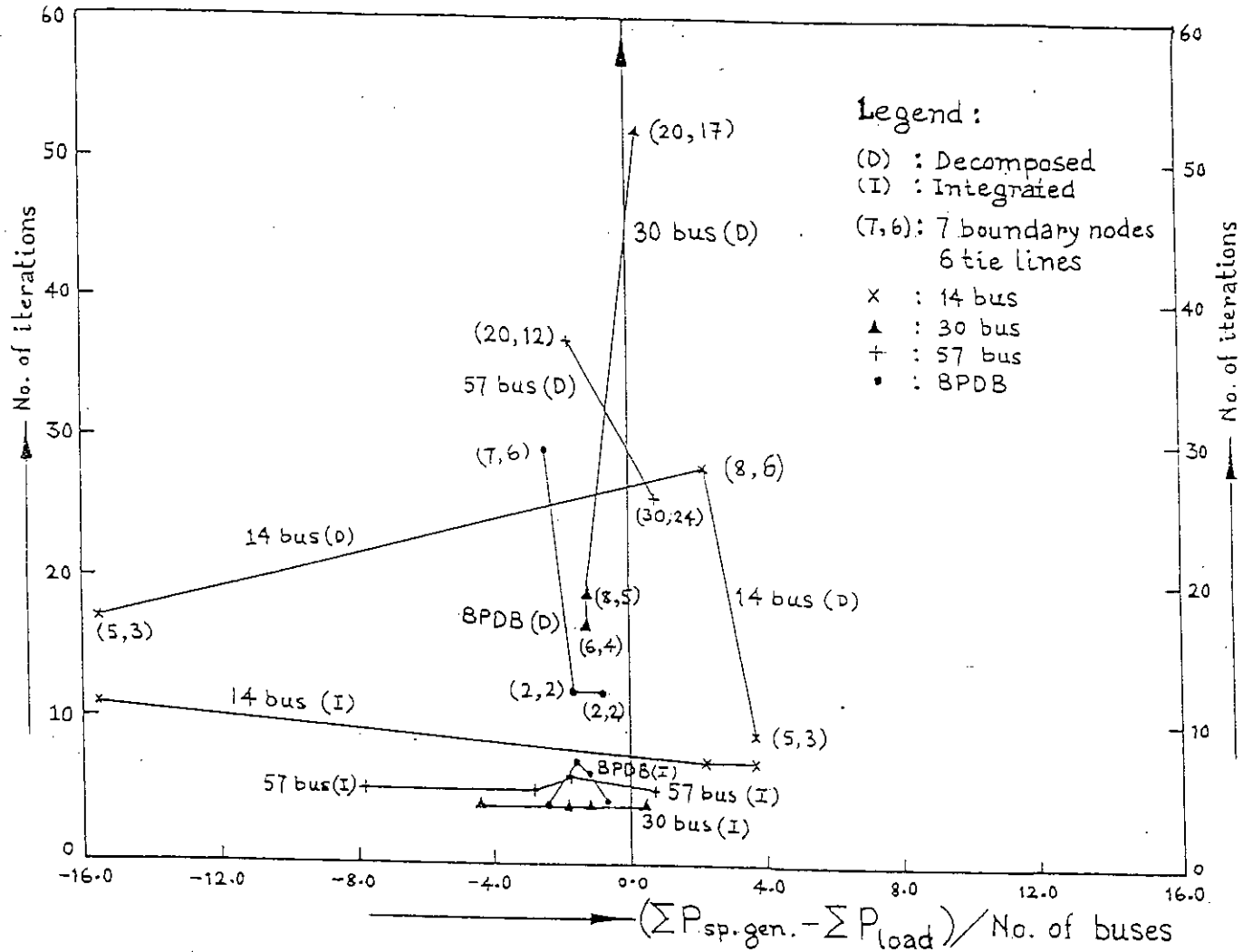


Figure 4.5 Convergence characteristics of the decomposed and integrated methods with the variation of average active power balance.

a consistency between the number of tie lines and boundary nodes and the amount of active power balance. In few cases the power balance was increasing i.e. having positive values but outweighed by an increase in the number of boundary nodes and tie lines so that the decomposed method either took more iterations to converge or did not converge even in 100 iterations. However, the decomposed method converged in most of the cases with a reasonable number of boundary nodes and tie lines against a practical value (deficit or surplus) of active power balance.

A comparison of the four convergence patterns of the decomposed method (corresponding to the four systems) among themselves shows that in terms of the number of iterations the decomposed method performed very well for the BPDB system which is the biggest one among the four and a practical one with naturally existing distinct geographical zones and reasonable number of tie lines and boundary nodes. All the cases of the BPDB system in which the decomposed method converged had a deficit in specified active power balance.

Figure 4.5 also shows that the decomposed method converged in 17 iterations even for an excessively high deficit case of active

power balance e.g. -15.59 MW/bus in 14 bus system with 5 boundary nodes and 3 tie lines. Also it converged for the cases with an excessively high number of boundary nodes and tie lines e.g. in 37 iterations for the case with 20 boundary nodes and 12 tie lines against a deficit balance of -2.29 MW/bus and in 26 iterations for the case with 30 boundary nodes and 24 tie lines against a slight positive balance of 0.828 MW/bus both in the 57 bus system.

The number of iterations required by the decomposed method to converge in various cases of the four test systems have been plotted against the active power mismatch at the boundary nodes in Figure 4.6. The total of the absolute mismatch value at each boundary node was expressed in percent of the total of the same at all the nodes of the system. In Figure 4.6 the curve has been drawn to best fit the points representing the various cases of the four systems. As may be seen in Figure 4.6 the general trend of the decomposed method was that the higher the number of iterations (above 17) it took for convergence in a case the more was the mismatch at the boundary nodes.

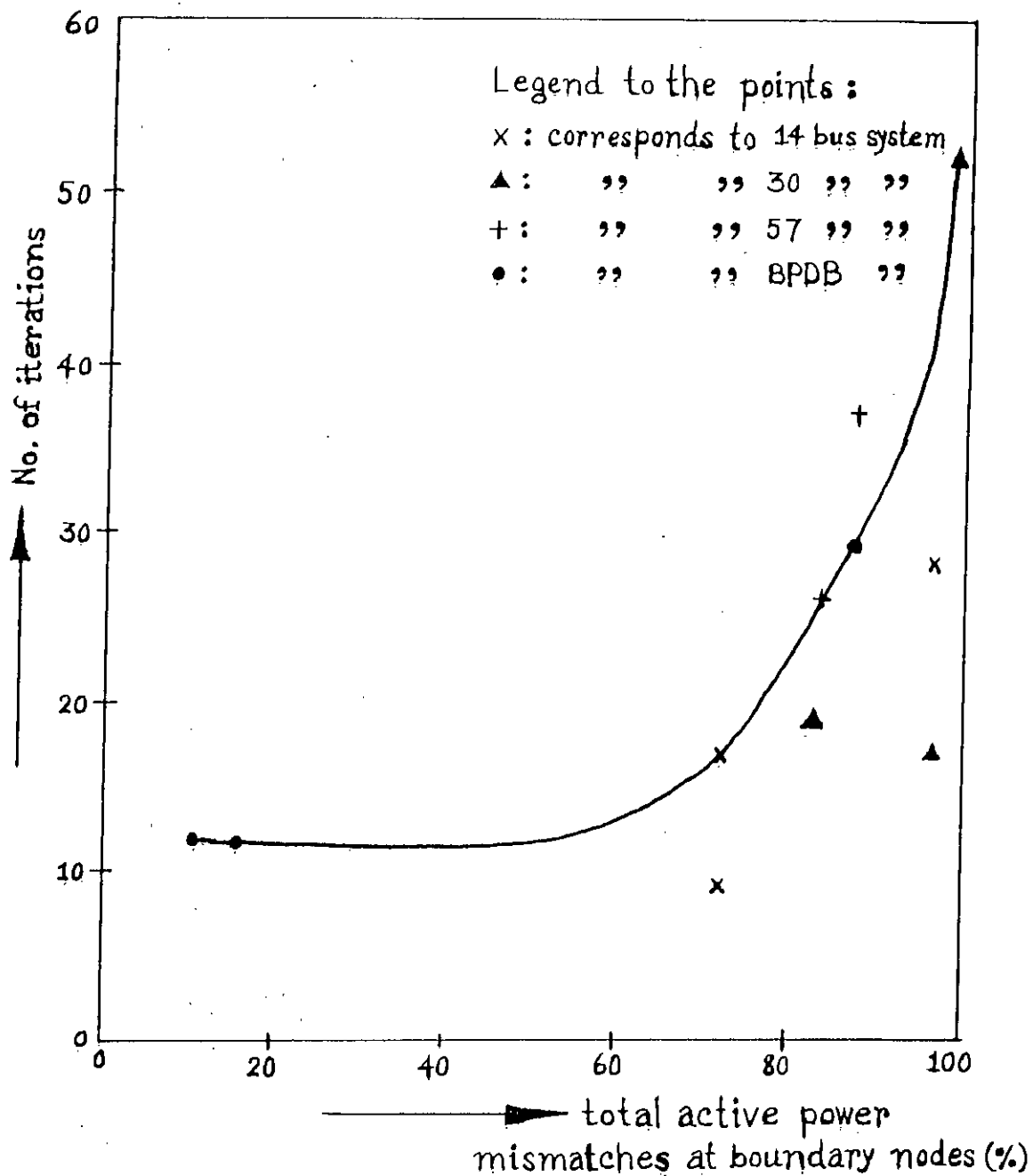


Figure 4.6

Iterations vs. boundary node mismatches of the decomposed method

#### 4.7 Comparison of CPU Time and Memory Requirement of the Decomposed and the Integrated Methods

87389  
The decomposed and the integrated methods both used fast decoupled Newton-Raphson load flow technique and exploited sparsity. The sparsity directed bifactorisation technique was used instead of direct inversion of the Jacobian matrices in both the methods. The only difference is that the decomposed method involved the subsystem Jacobian matrices and solution vectors of an order equal to the number of nodes in the respective subsystem while the integrated method involved the Jacobian matrix and the solution vector of an order equal to the number of nodes in the whole system. As mentioned in section 2.3 the sparse matrix technique consists of four distinct steps : compacting, ordering, bifactorisation and solution. The computation (CPU) time needed for each of them increases in proportion to a number of variables viz : the number of nodes and branches in the system or subsystem and the initial and final number of nonzero elements of the Jacobian matrix so that the increase is not exactly linear. The fast decoupled load flow technique has two major components of computations : fixed and iterative. Fixed calculations need to be done only once for a given system or subsystem prior to iterative calculations and refers to mainly formation, compacting, ordering

and factorisation of the system or subsystem active and reactive power Jacobian matrices. Iterative computations need to be done in each iteration and refers to mainly solution i.e. updating the phase angle and voltage magnitude vectors by multiplying the calculated injection vectors by the corresponding bifactorised Jacobian matrix.

Table 4.6 shows a breakup of the CPU time needed for fixed and iterative computations for the decomposed and the integrated methods corresponding to a pair of converged cases of each test system shown in Table 4.5. The pair represents respectively the case with the highest and the case with the lowest number of iterations required for convergence of the decomposed method.

In Table 4.6 the total CPU time was calculated by adding time for fixed computations to the time for iterative computations i.e. the product of time per iteration and number of iterations. The case nos. given against each system in Table 4.6 corresponds to those shown in Table 4.5.



Table 4.6 : Comparison of CPU time for the decomposed and the integrated fast decoupled methods using sparse matrix technique on an IBM 4331 computer

System	No. of branches in the whole system	Case No.	Integrated method CPU time (sec.)				Decomposed method CPU time (sec.)				
			time for fixed calculations	time/iteration	No. of iterations	total time	No. of iterations	Subsystems	time for fixed calculations	time/iteration	total time
14 Bus	20	II	1.0	0.6	7	1.42	9	1 (5 nodes)	0.25	0.01	0.34
								2 (9 nodes)	0.30	0.01	0.39
		III	1.0	0.6	7	1.42	28	1 (7 nodes)	0.27	0.01	0.55
								2 (7 nodes)	0.27	0.01	0.55
30 Bus	41	I	3.0	0.1	4	3.4	17	1 (25 nodes)	1.3	0.06	2.32
								2 (5 nodes)	0.26	0.01	0.43
		III	3.0	0.1	4	3.4	52	1 (12 nodes)	0.4	0.015	1.18
								2 (12 nodes)	0.4	0.015	1.18
							3 (6 nodes)	0.25	0.01	0.77	
57 Bus	80	I	6.0	0.18	6	7.08	37	1 (16 nodes)	0.8	0.02	1.54
								2 (41 nodes)	3.5	0.1	7.2
		II	6.0	0.18	5	6.9	26	1 (10 nodes)	0.3	0.01	0.56
								2 (30 nodes)	2.6	0.07	4.42
							3 (17 nodes)	1.0	0.02	1.52	
BPDB (81 Bus)	114	I	10.0	0.3	7	12.1	12	1 (51 nodes)	4.0	0.15	5.80
								2 (30 nodes)	2.8	0.1	2.92
		III	10.0	0.3	4	11.2	29	1 (20 nodes)	1.0	0.056	2.624
								2 (31 nodes)	2.8	0.1	3.09
							3 (30 nodes)	2.8	0.1	3.09	

In on-line mode if the decomposed algorithm is implemented on a single computer performing the computations of all the subsystems sequentially then the actual CPU time would be sum of subsystem total times shown in Table 4.6. In that case the decomposed method's time required will be still less than that of the integrated method expecting for a case like case No. I of the 57 bus system in which it is more by about 1.6 seconds. But it should be noted that the 14, 30 and 57 bus systems are hypothetical small test systems with a densely connected topology more vulnerable to integrated analysis. On the otherhand the BPDB system is a practical one and this one like other interconnected or large-scale systems is more amenable to decomposed analysis. However, the total on-line CPU time of the decomposed method implemented on a single computer varies on the average from 51% to 72% of the integrated method's time for the various cases of the four power test systems.

If the decomposed algorithm is implemented in a multiprocessor environment i.e. same computer memory shared by a number of processors (CPU units) one for each subsystem or in a multicomputer environment i.e. one independent computer for each subsystem then parallel processing would be possible. In this case the

actual CPU time of the decomposed method would be that of the slowest subsystem requiring the highest total time as shown in Table 4.6. Then the decomposed method's time requirement varies on the average from 24% to 64% of the integrated method's time for the four test systems. For the BPDB system in particular this percentage is only 27% to 47%. Also the higher the number of subsystems the more would be the saving of CPU time requirement of the decomposed method in multiprocessor or multicomputer environment. However, for the multicomputer environment the data on boundary node bus voltage magnitudes and phase angles are to be exchanged among the subsystem computers in each iteration. But the amount of this data transfer is too nominal to be reckoned for modern speedy data communication systems. For the multiprocessor environment housing all the processors in the same place no data transfer is no required.

As regards the memory requirement, it should be noted that the program area is the same for both the methods. For data area the integrated method needs more space depending upon the size of the whole system while the decomposed method's data area depends upon the highest sized subsystem.

In simulation stage however, the program length of the decomposed method was slightly more e.g. about 1600 lines against 1100 lines of integrated method's program. This is because an integrated system was decomposed into a number of subsystems and the nodes and lines were renumbered in terms of the serial numbers in respective subsystem. Moreover, the various arrays were to be shared by the subsystems.

As regards the advantage of the proposed algorithm of the decomposed method over the existing algorithms it should be noted that the proposed one does not need any further coordinations or computations after the subsystem level solutions while the existing versions do so involving matrix operations and other computations of an order equal to either the number of tie lines and/or boundary nodes. The further CPU time needed by the existing version for this can be perceived from an example. If the 57 bus system case no. II with 30 boundary nodes and 24 tie lines were to be solved by the existing decomposed algorithms then operation of matrices of size  $30 \times 30$  and/or  $24 \times 24$  would have been involved. Moreover, reupdating 57 bus variables in each iteration was also necessary. So the proposed algorithm saves an equivalent CPU time which otherwise adds to the slowest subsystem's time or to the total of all the

subsystem times respectively in multiprocessor/multicomputer or single computer implementation mode for the existing decomposed algorithms.

#### 4.8 Conclusions

The proposed decomposed load flow algorithm has been tested extensively on three IEEE test systems (14, 30 and 57 bus) and one practical system (81 bus BPDB) of diverse size and characteristics with various operating conditions and compared against the integrated method in terms of mismatch, number of iterations, computer time and memory requirement. Both the decomposed and the integrated methods used sparsity exploited fast decoupled Newton-Raphson load flow technique.

The mismatches produced and iterations required by the decomposed method were more than those of the integrated method due to the former's inherent characteristic of confining each node's injection within the subsystem to which it belongs. However, these were within acceptable limit. The mismatches at the boundary nodes mainly constituted the major percentage of the total mismatches at all the nodes in those cases where the decomposed method required more than 17 iterations.

In general, the convergence characteristics of the decomposed method was influenced combinedly by specified active power balance, number of tie lines and boundary nodes. With an increasing balance the number of iterations decreased provided the increase was not offset by an increase in the number of tie lines and boundary nodes.

As regards the CPU time, the decomposed method requires 51% to 72% of the integrated method's time when implemented on a single computer performing computations of all the subsystems sequentially. When it is implemented in a multiprocessor or multicomputer environment allowing parallel processing of subsystems' computations it requires only 24% to 64% of the time taken by the integrated method depending upon the system size, topological structure and number of subsystems. The data transfer needed in multicomputer environment is also very nominal. Also the memory requirement of the proposed technique is the same as that of the integrated method for the program area while much less than that of the latter for the data area depending upon the size of the subsystems into which a system is divided.

It has been observed that the practical large systems like the BPDB system are more amenable to the decomposed load flow analysis than the smaller and densely connected hypothetical test systems like 14, 30 and 57 bus systems.

The main advantage of the proposed version over the existing versions of the decomposed load flow method is that it does not require coordination of the subsystem solutions through a separate tie model and hence saves an extra CPU time. This saving is very much significant when it is noted that the proposed decomposed algorithm was successful in solving a case of the densely connected 57 bus system with 30 boundary nodes and 24 tie lines.

**CHAPTER 5**  
**CONCLUSIONS**



## 5.1 Conclusions

Load flow analysis is one of the well-known mathematical tools for the modelling, simulation and analysis of various operational aspects of a power system. This provides the steady state profile of a system's unknown bus voltages, phase angles, generation and line flows from a set of specified power injection and voltages. Since the beginning, load flow analysis of a system is being done considering the system in a single piece i.e. using an integrated approach. With the continued growth in demand for electricity and hence an increase in system size as well as a tendency to interconnect two or more utilities, research effort has been put on reducing the dimensionality problem and enhancing the on-line compatibility of the integrated load flow analysis. These include model decoupling i.e. neglecting the dependence of active power upon voltage magnitude and reactive power upon phase angle and exploitation of the sparse network topology of the power system in forming the Jacobian matrix. However, a second approach has also been developed for load flow analysis of a large scale power system. This approach called decomposed load flow analysis treats a system dividing it into a number of subsystems chosen suitably based on already existent geographical zones or some other functional considerations. It has been found that use of sparsity

exploitation and model decoupling with the integrated approach can not satisfy the standard set for the computational performance for the present day's real time control strategies, rather use of these techniques together with system decomposition is more effective and preferable.

In this project work a version of the decomposed load flow analysis has been developed in which the Jacobian matrix is formed for each subsystem of its own. Its coupling with other subsystem through tie lines is considered including the admittances only in the diagonal elements corresponding to the ends of the tie lines in the subsystem under consideration. The overall structure of the whole system Jacobian matrix then assumes a completely block diagonal form such that each diagonal block represents a subsystem while the off-diagonal blocks are null representing decoupling of the subsystems from each other. For this the proposed version can be termed space decoupled version of decomposed load flow analysis. The main advantage of the proposed version over existing versions is performing each subsystem's solution independently at the same time on a multiprocessor / multicomputer implementation or separately one after another on a single computer without requiring further coordination or reupdating the solutions through tie line

model in any mode of implementation. This saves the extra CPU time for manipulating the tie line model separately as required in the existing versions.

The proposed decomposed technique has been compared against the integrated method extensively using three IEEE test systems (14, 30 and 57 bus) and a practical network (81 bus BPDB system) with various operating characteristics. Both the methods used fast decoupled Newton-Rapson load flow analysis and sparse matrix bifactorisation technique. Though the mismatch and number of iterations of the decoupled method were more (but acceptable) than those of the integrated method it compared favourably in terms of CPU time and memory requirement in general for all the systems and more particularly for the BPDB network which is a representative of the practical large scale / interconnected systems.

## 5.2 Suggestions for Further Research

The proposed decomposed technique confines the effect of injection at each node only within the subsystem to which the node belongs, due to space decoupling in the Jacobian matrix. On the otherhand the integrated method spreads the effects of injection at each node to all other nodes whether connected directly or not, due

to the treatment of the whole system as a single piece by the integrated method. So if the missing contributions from the nodes in other subsystems can be compensated in each iteration by adding an equivalent quantity with the solution variables particularly the phase angles of a subsystem, the advantages of completely block diagonal Jacobian matrix structure and at the same time a reduced number of iterations for convergence would have been obtained by the proposed decomposed method. Investigating into determining this equivalent quantity could be an interesting point for further research.

## REFERENCES

1. G. T. Heydt, "Computer Analysis Methods for Power Systems", Macmillan Publishing Company, New York, 1986, pp. 77-169.
2. J. Arrillaga, C. P. Arnold and B. J. Harker, "Computer Modelling of Electrical Power Systems", John Wiley and Sons, U. K., 1983, pp. 58-89.
3. K. Zollenkopf, "Bifactorisation-Basic Computational Algorithm and Programming Techniques", Proceedings of the conference on large sets of linear equations, Oxford, U. K., 1970, pp.75-96.
4. H. H. Happ, "Piecewise Methods and Applications to Power Systems", John Wiley and Sons, New York, 1980, pp. 368-382.
5. M. EL-Marsafawy, R. W. Menzies and R. M. Mathur, "A New, Exact, Diakoptic, Fast Decoupled Load Flow Technique for Very Large Power Systems", Paper No. A 79 440-9, presented at the 1979 IEEE Summer Meeting.
6. M. R. Rafian and M. J. H. Sterling, "Multi-processor Decomposed Load Flow", IEE Conference publication no. 226, 2nd international conference on power system monitoring and control, 8-11 July 1986, Durham, U. K., pp. 256-260.

## **APPENDICES**

**APPENDIX A**  
**IEEE 14 BUS SYSTEM DATA**



**IEEE 14 Bus System Data**  
 (Operating conditions correspond to case I)

Base MVA = 100, Slack bus No. 1  
 Bus data

Node no.	Specified voltage (p.u.)	Specified generation		Specified load	
		P (MW)	Q (MVAR)	P (MW)	Q (MVAR)
1	1.06	-	-	-	-
2	1.045	40	-	21.0	12.7
3	1.010	-	-	94.2	19.0
4	-	-	-	47.8	3.9
5	-	-	-	7.6	1.6
6	1.060	-	12.2	11.2	7.5
7	-	-	-	-	-
8	1.080	-	17.4	-	-
9	-	-	-	29.5	16.6
10	-	-	-	9.0	5.8
11	-	-	-	3.5	1.8
12	-	-	-	6.1	1.6
13	-	-	-	13.5	5.8
14	-	-	-	14.9	5.0

Line data

Sending end node no.	Receiving end node no.	Resistance (p.u.)	Reactance (p.u.)	Susceptance (p.u.)
1	2	0.0193	0.0591	0.0528
2	3	0.4699	0.1979	0.0438
2	4	0.0581	0.1763	0.0374
1	5	0.0540	0.2230	0.0492
2	5	0.0569	0.1738	0.0340
3	4	0.0670	0.1710	0.0340
4	5	0.0133	0.0421	0.0128
5	6	-	0.2520	-
4	7	-	0.2091	-
7	8	-	0.1761	-
4	9	-	0.5561	-
7	9	-	0.1100	-
9	10	0.0318	0.0845	-
6	11	0.0949	0.1989	-
6	12	0.1229	0.2558	-
6	13	0.0661	0.1302	-
9	14	0.1271	0.2703	-
10	11	0.0820	0.1920	-
12	13	0.2209	0.1998	-
13	14	0.1709	0.348	-
9	9	-	-5.126	-

**APPENDIX B**  
**IEEE 30 BUS SYSTEM DATA**

**IEEE 30 Bus System Data**  
(Operating conditions correspond to case I)

Base MVA = 100, Slack bus No. 1

**Bus data**

Node no.	Specified voltage  (p.u.)	Specified generation		Specified load	
		P (MW)	Q (MVAR)	P (MW)	Q (MVAR)
1	1.050	-	-	-	-
2	1.034	57.56	-	21.7	12.7
3	-	-	-	2.4	1.2
4	-	-	-	7.6	1.6
5	1.006	24.56	-	94.2	19.0
6	-	-	-	-	-
7	-	-	-	22.8	10.9
8	1.023	35.0	-	30.0	30.0
9	-	-	-	-	-
10	-	-	-	5.8	2.0
11	1.091	17.93	-	-	-
12	-	-	-	11.2	7.5
13	1.088	16.91	-	-	-
14	-	-	-	6.2	1.6
15	-	-	-	8.2	2.5
16	-	-	-	3.5	1.8
17	-	-	-	9.0	5.8
18	-	-	-	3.2	0.9
19	-	-	-	9.5	3.4
20	-	-	-	2.2	0.7
21	-	-	-	17.5	11.2
22	-	-	-	-	-
23	-	-	-	3.2	1.6
24	-	-	-	8.7	6.7
25	-	-	-	-	-
26	-	-	-	3.5	2.3
27	-	-	-	-	-
28	-	-	-	-	-
29	-	-	-	2.4	0.9
30	-	-	-	10.6	1.9

Line data

Sending end node no.	Receiving end node no.	Resistance (p.u.)	Reactance (p.u.)	Susceptance (p.u.)
1	2	0.0192	0.0575	0.0528
1	3	0.0452	0.1852	0.0408
2	4	0.0570	0.1737	0.0368
3	4	0.0132	0.0379	0.0084
2	5	0.0472	0.1983	0.0418
2	6	0.0581	0.1763	0.0374
4	6	0.0119	0.0414	0.0090
5	7	0.0460	0.1160	0.0204
6	7	0.0267	0.0820	0.0170
6	8	0.0120	0.0420	0.0090
6	9	-	0.2080	-
6	10	-	0.5560	-
9	11	-	0.2080	-
9	10	-	0.1100	-
4	12	-	0.2560	-
12	13	-	0.1400	-
12	14	0.1231	0.2559	-
12	15	0.0662	0.1304	-
12	16	0.0945	0.1987	-
14	15	0.2210	0.1997	-
16	17	0.0824	0.1932	-
15	18	0.1070	0.2185	-
18	19	0.0639	0.1292	-
19	20	0.0340	0.0680	-
10	20	0.0936	0.2090	-
10	17	0.0324	0.0845	-
10	21	0.0348	0.0749	-
10	22	0.0727	0.1499	-
21	22	0.0116	0.0236	-
15	23	0.1000	0.2020	-
22	24	0.1150	0.1790	-
23	24	0.1320	0.2700	-
24	25	0.1885	0.3292	-
25	26	0.2544	0.3800	-
25	27	0.1093	0.2087	-
26	27	-	0.3960	-

Line data (Continued)

Sending end node no.	Receiving end node no.	Resistance (p.u.)	Reactance (p.u.)	Susceptance (p.u.)
27	29	0.2198	0.4153	-
27	30	0.3202	0.6027	-
29	30	0.2399	0.4533	-
8	28	0.0636	0.2000	0.0428
6	28	0.0169	0.0599	0.0130
10	10	-	-5.263	-
24	24	-	-25.0	-

**APPENDIX C**  
**IEEE 57 BUS SYSTEM DATA**

IEEE 57 Bus System Data  
(Operating conditions correspond to case I)

Base MVA = 100, Slack bus No. 1

Bus data

Node no.	Specified voltage (p.u.)	Specified generation		Specified load	
		P (MW)	Q (MVAR)	P (MW)	Q (MVAR)
1	1.040	-	-	55.0	17.0
2	1.010	-	-	3.0	88.0
3	0.985	40.0	-	41.0	21.0
4	-	-	-	-	-
5	-	-	-	13.0	4.0
6	0.980	-	-	75.0	2.0
7	-	-	-	-	-
8	1.005	450.0	-	150.0	22.0
9	0.980	-	-	121.0	26.0
10	-	-	-	5.0	2.0
11	-	-	-	-	-
12	1.015	310.0	-	377.0	24.0
13	-	-	-	18.0	2.3
14	-	-	-	10.5	5.3
15	-	-	-	22.0	5.0
16	-	-	-	43.0	3.0
17	-	-	-	42.0	8.0
18	-	-	-	27.2	9.8
19	-	-	-	3.3	0.6
20	-	-	-	2.3	1.0
21	-	-	-	-	-
22	-	-	-	-	-
23	-	-	-	6.3	2.1
24	-	-	-	-	-
25	-	-	-	6.3	3.2
26	-	-	-	-	-
27	-	-	-	9.3	0.5
28	-	-	-	4.6	2.3
29	-	-	-	17.0	2.6
30	-	-	-	3.6	1.8
31	-	-	-	5.8	2.9



Bus data (Continued)

Node no.	Specified voltage  (p.u.)	Specified generation		Specified load	
		P (MW)	Q (MVAR)	P (MW)	Q (MVAR)
32	-	-	-	1.6	0.8
33	-	-	-	3.8	1.9
34	-	-	-	-	-
35	-	-	-	6.0	3.0
36	-	-	-	-	-
37	-	-	-	-	-
38	-	-	-	14.0	7.0
39	-	-	-	-	-
40	-	-	-	-	-
41	-	-	-	6.3	3.0
42	-	-	-	7.1	4.0
43	-	-	-	2.0	1.0
44	-	-	-	12.0	1.8
45	-	-	-	-	-
46	-	-	-	-	-
47	-	-	-	29.7	11.6
48	-	-	-	-	-
49	-	-	-	18.0	8.5
50	-	-	-	21.0	10.5
51	-	-	-	18.0	5.3
52	-	-	-	4.9	2.2
53	-	-	-	20.0	10.0
54	-	-	-	4.1	1.4
55	-	-	-	6.80	3.4
56	-	-	-	7.6	2.2
57	-	-	-	6.7	2.0

Line data

Sending end node no.	Receiving end node no.	Resistance (p.u.)	Reactance (p.u.)	Susceptance (p.u.)
1	2	0.0083	0.0280	0.1290
2	3	0.0298	0.0850	0.0818
3	4	0.0112	0.0366	0.0380
4	5	0.0625	0.1320	0.0258
4	6	0.0430	0.1480	0.0348
6	7	0.0200	0.1020	0.0276
6	8	0.0339	0.1730	0.0470
8	9	0.0099	0.0505	0.0548
9	10	0.0369	0.1679	0.0440
9	11	0.0258	0.0848	0.0218
9	12	0.0648	0.2950	0.0772
9	13	0.0481	0.1580	0.0406
13	14	0.0132	0.0434	0.0110
13	15	0.0269	0.0869	0.0230
1	15	0.0178	0.0910	0.0988
1	16	0.0454	0.2060	0.0546
1	17	0.0238	0.1080	0.0286
3	15	0.0162	0.0530	0.0544
4	18	-	0.5550	-
4	18	-	0.4300	-
5	6	0.0302	0.0641	0.0124
7	8	0.0139	0.0712	0.0194
10	12	0.0277	0.1262	0.0328
11	13	0.0223	0.0732	0.0188
12	13	0.0178	0.0580	0.0604
12	16	0.0180	0.0813	0.0216
12	17	0.0397	0.1790	0.0476
14	15	0.0171	0.0547	0.0148
18	19	0.4610	0.6850	-
19	20	0.2830	0.4340	-
20	21	-	0.7767	-
21	22	0.0736	0.1170	-
22	23	0.0099	0.0152	-
23	24	0.1660	0.2560	0.0084
24	25	-	0.1820	-

Line data (Continued)

Sending end node no.	Receiving end node no.	Resistance (p.u.)	Reactance (p.u.)	Susceptance (p.u.)
24	25	-	1.2300	-
24	26	-	0.0473	-
26	27	0.1650	0.2540	-
27	28	0.0618	0.0954	-
28	29	0.0418	0.0587	-
7	29	-	0.0648	-
25	30	0.1350	0.0202	-
30	31	0.3260	0.4970	-
31	32	0.5070	0.7550	-
32	33	0.0392	0.0360	-
32	34	-	0.9530	-
34	35	0.0520	0.0780	0.0032
35	36	0.0430	0.0537	0.0016
36	37	0.0290	0.0366	-
37	38	0.0651	0.1009	0.0020
37	39	0.0239	0.0379	-
36	40	0.0300	0.0466	-
22	38	0.0192	0.0295	-
11	41	-	0.7490	-
41	42	0.2070	0.3520	-
41	43	-	0.4120	-
38	44	0.0289	0.0585	0.0020
15	45	-	0.1042	-
14	46	-	0.0735	-
46	47	0.0230	0.0680	0.0032
47	48	0.0182	0.0233	-
48	49	0.0834	0.1290	0.0048
49	50	0.0801	0.1280	-
50	51	0.1386	0.2200	-
10	51	-	0.0712	-
13	49	-	0.1910	-
29	52	0.1442	0.1870	-
52	53	0.0762	0.0984	-
53	54	0.1878	0.2320	-
54	55	0.1732	0.2265	-

Line data (Continued)

Sending end node no.	Receiving end node no.	Resistance (p.u.)	Reactance (p.u.)	Susceptance (p.u.)
11	43	-	0.1530	-
44	45	0.0624	0.1242	0.0040
40	56	-	0.1950	-
56	41	0.5530	0.5490	-
56	42	0.2125	0.3540	-
39	57	-	0.3550	-
57	56	0.1740	0.2600	-
38	49	0.1150	0.1770	0.0060
38	48	0.0312	0.0482	-
9	55	-	0.1205	-
18	18	-	-10.07	-
25	25	-	-16.95	-
53	53	-	-15.87	-

**APPENDIX D**  
**BPDB 81 BUS GRID SYSTEM DATA**

**BPDB Grid System**  
(Operating Conditions correspond to Case I)

Base MVA = 100, Slack bus No. 12

**Bus data**

Node no.	Specified voltage (p.u.)	Specified generation		Specified load	
		P (MW)	Q (MVAR)	P (MW)	Q (MVAR)
1	1.03	20	15	1.4	0.7
2	1.03	95	80	3.0	1.5
3	-	-	-	72.8	35.3
4	-	-	-	73.7	35.7
5	-	-	-	38.2	18.5
6	-	-	-	77.2	37.4
7	-	-	-	70.7	34.3
8	-	-	-	61.0	29.6
9	-	-	-	16.0	7.8
10	-	-	-	22.4	10.9
11	1.05	150	140	7.5	3.7
12	1.05	210	170	15.0	7.0
13	-	-	-	-	-
14	-	-	-	44.7	21.7
15	1.03	95	75	15.0	7.0
16	-	-	-	-	-
17	1.03	60	40	4.2	2.1
18	1.03	55	40	2.0	1.0
19	1.03	30	20	2.0	1.0
20	-	-	-	-	-
21	-	-	-	21.5	10.4
22	1.03	-	-	-	-
23	1.03	130	100	11.0	5.4
24	1.03	130	100	11.0	5.4
25	1.03	130	100	11.0	5.4
26	-	-	-	12.3	6.0
27	-	-	-	24.3	11.8
28	-	-	-	13.6	6.6
29	-	-	-	7.2	3.5
30	1.03	20	17	0.5	0.25
31	-	-	-	19.7	9.6

Bus data (Continued)

Node no.	Specified voltage  (p.u.)	Specified generation		Specified load	
		P (MW)	Q (MVAR)	P (MW)	Q (MVAR)
32	-	-	-	7.0	3.4
33	-	-	-	10.0	4.8
34	-	-	-	7.0	3.4
35	1.03	-	-	-	-
36	1.03	80	55	1.5	0.75
37	1.03	40	30	0.8	0.4
38	1.03	95	65	1.5	0.75
39	-	-	-	-	-
40	-	-	-	18.9	8.9
41	-	-	-	-	-
42	-	-	-	50.0	24.2
43	-	-	-	61.7	29.9
44	-	-	-	40.0	19.4
45	-	-	-	6.2	3.0
46	-	-	-	14.8	7.2
47	1.03	75	55	5.2	2.6
48	-	-	-	35.0	17.0
49	-	-	-	31.3	15.2
50	-	-	-	34.9	16.9
51	-	-	-	9.7	4.7
52	-	-	-	-	-
53	-	-	-	26.4	12.8
54	-	-	-	33.0	16.0
55	-	-	-	8.7	4.2
56	-	-	-	22.8	11.0
57	1.03	20	15	1.0	0.5
58	-	-	-	21.0	0.2
59	1.03	12	15	1.0	0.5
60	-	-	-	13.0	6.3
61	-	-	-	13.0	6.3
62	-	-	-	29.7	4.4
63	-	-	-	8.9	4.3
64	-	-	-	10.3	5.2
65	-	-	-	16.0	7.8
66	1.03	-	45	1.4	0.7

Bus data (Continued)

Node no.	Specified voltage (p.u.)	Specified generation		Specified load	
		P (MW)	Q (MVAR)	P (MW)	Q (MVAR)
67	-	-	-	21.9	0.6
68	-	-	-	18.9	9.2
69	-	-	-	10.2	4.9
70	-	-	-	70.4	4.1
71	-	-	-	1.8	0.9
72	1.03	40	40	7.0	3.4
73	1.03	-	-	-	-
74	1.03	20	18	0.8	0.4
75	-	-	-	2.0	1.0
76	-	-	-	13.0	6.3
77	1.03	-	40	1.5	0.75
78	-	-	-	22.5	10.9
79	-	-	-	10.5	5.1
80	-	-	-	13.7	6.6
81	-	-	-	35.0	17.0

Line data

Sending end node no.	Receiving end node no.	Resistance (p.u.)	Reactance (p.u.)	Susceptance (p.u.)
3	14	0.0258	0.0946	0.0236
3	14	0.0258	0.0946	0.0236
3	4	0.0089	0.0363	0.0073
3	8	0.0261	0.1234	0.0250
39	40	0.0047	0.0177	0.0041
39	42	0.0226	0.0861	0.0200
39	41	0.0222	0.0258	0.0202
39	41	0.0222	0.0258	0.0202
40	42	0.0179	0.0688	0.0159
42	45	0.0094	0.0348	0.0085



Line data (Continued)

Sending end node no.	Receiving end node no.	Resistance (p.u.)	Reactance (p.u.)	Susceptance (p.u.)
42	45	0.0094	0.0348	0.0085
42	43	0.0074	0.0301	0.0061
42	43	0.0074	0.0301	0.0061
42	41	0.0050	0.0186	0.0046
42	41	0.0050	0.0186	0.0046
41	49	0.0515	0.1812	0.0474
49	50	0.0282	0.1046	0.0259
41	50	0.0798	0.2958	0.0733
45	44	0.0086	0.0293	0.0058
45	46	0.0188	0.0717	0.0165
41	48	0.0070	0.0258	0.0064
41	48	0.0070	0.0258	0.0064
43	44	0.0079	0.0321	0.0065
43	48	0.0075	0.0309	0.0061
50	3	0.0510	0.1888	0.0468
50	3	0.0510	0.1888	0.0468
50	51	0.0672	0.1431	0.0298
4	5	0.0031	0.0034	0.1054
4	5	0.0031	0.0034	0.1054
4	6	0.0112	0.0427	0.0099
4	6	0.0112	0.0427	0.0099
6	8	0.0084	0.0342	0.0069
6	7	0.0251	0.1026	0.0207
7	3	0.0124	0.0055	0.0112
6	9	0.0123	0.0464	0.0109
14	21	0.0254	0.0932	0.0232
14	21	0.0254	0.0932	0.0232
9	10	0.0208	0.1130	0.0265
21	34	0.0302	0.1112	0.0232
21	34	0.0302	0.1112	0.0232
34	33	0.0212	0.0806	0.0188
33	32	0.0286	0.1087	0.0254
32	31	0.0183	0.0697	0.0162
31	29	0.0187	0.0720	0.0166
21	26	0.0301	0.1143	0.0269

Line data (Continued)

Sending end node no.	Receiving end node no.	Resistance (p.u.)	Reactance (p.u.)	Susceptance (p.u.)
26	27	0.0343	0.1299	0.0305
27	28	0.0321	0.1211	0.0284
71	70	0.0006	0.0018	0.0091
71	70	0.0006	0.0018	0.0091
70	69	0.0168	0.0491	0.0109
70	69	0.0168	0.0491	0.0109
69	81	0.0124	0.0566	0.0126
69	68	0.0543	0.1585	0.0353
81	65	0.0861	0.2511	0.0559
68	67	0.0837	0.0983	0.0291
67	65	0.0175	0.0509	0.0113
65	53	0.0074	0.0212	0.0049
65	53	0.0074	0.0212	0.0049
71	76	0.0886	0.1050	0.0204
76	78	0.0515	0.1609	0.0312
76	75	0.0244	0.0762	0.0148
78	79	0.0437	0.1294	0.0280
79	80	0.0499	0.1480	0.0320
80	65	0.0809	0.2400	0.0521
63	54	0.0518	0.1511	0.0338
53	63	0.0275	0.0799	0.0179
53	54	0.0793	0.2310	0.0517
63	62	0.0311	0.0948	0.0193
54	55	0.0382	0.1134	0.0254
54	55	0.0382	0.1134	0.0254
55	56	0.0407	0.1184	0.0265
55	56	0.0407	0.1184	0.0265
56	58	0.0318	0.0926	0.0208
56	58	0.0318	0.0926	0.0208
58	60	0.0162	0.0474	0.0105
60	61	0.0387	0.0983	0.0219
53	64	0.0553	0.1705	0.0347
20	16	0.0107	0.0507	0.1095
20	16	0.0107	0.0507	0.1095
13	52	0.0272	0.1304	0.2778
13	52	0.0272	0.1304	0.2778

Step-up transformers data

Sending end node no.	Receiving end node no.	Reactance (p.u.)
36	36	0.1111
37	39	0.2260
38	39	0.0880
47	45	0.0876
1	3	0.1221
2	3	0.1000
17	20	0.1100
18	20	0.1700
19	20	0.3660
22	21	0.1700
23	21	0.0700
24	21	0.0700
25	21	0.0700
15	14	0.0835
12	13	0.0450
11	13	0.0450
35	34	0.0800
30	31	0.4428
72	71	0.0950
73	71	0.1486
74	71	0.2243
77	78	0.1500
66	65	0.1405
59	58	0.4430
57	56	0.5337

### Inter-bus transformers data

Sending end node no.	Receiving end node no.	Reactance (p.u.)
20	21	0.1057
20	21	0.1057
13	13	0.0774
13	14	0.0774
16	6	0.0577
16	6	0.0577
52	53	0.0577
52	53	0.0577

